

21\_104\_3  
FH reports

## Morphodynamic modelling of the Belgian Coastal zone

Sub report 3 – Implementation and testing cross-shore  
transport processes in GAIA

# Morphodynamic modelling of the Belgian Coastal zone

## Sub report 3 – Implementation and testing cross-shore transport processes in GAIA

Kolokythas, G.; Breugem, A.; De Maerschalck, B.

## Legal notice

Flanders Hydraulics is of the opinion that the information and positions in this report are substantiated by the available data and knowledge at the time of writing.

The positions taken in this report are those of Flanders Hydraulics and do not reflect necessarily the opinion of the Government of Flanders or any of its institutions.

Flanders Hydraulics nor any person or company acting on behalf of Flanders Hydraulics is responsible for any loss or damage arising from the use of the information in this report.

## Copyright and citation

© The Government of Flanders, Department of Mobility and Public Works, Flanders Hydraulics 2024  
D/2024/3241/101

This publication should be cited as follows:

**Kolokythas, G.; Breugem, A.; De Maerschalck, B.** (2024). Morphodynamic modelling of the Belgian Coastal zone: Sub report 3 – Implementation and testing cross-shore transport processes in GAIA. Version 4.0. FH Reports, 21\_104\_3. Flanders Hydraulics: Antwerp


Reproduction of and reference to this publication is authorised provided the source is acknowledged correctly.

## Document identification

Customer:	Flanders Hydraulics	Ref.:	WL2024R21_104_3
Keywords (3-5):	Coastal modelling, sediment transport, Cross-shore sediment transport		
Knowledge domains:	Hydraulics and sediment > Hydrodynamics > Waves > Numerical modelling Hydraulics and sediment > Hydrodynamics > Tides > Numerical modelling Hydraulics and sediment > Sediment > Sediment transport > Numerical modelling		
Text (p.):	31	Appendices (p.):	/
Confidential:	<input checked="" type="checkbox"/> No <input checked="" type="checkbox"/> Available online		

Author(s):	Kolokythas, G.
------------	----------------

## Control

	Name	Signature
Reviser(s):	Breugem, A.	Getekend door: Willem Breugem (Signatur) Getekend op: 2024-12-17 10:20:01 +01:0 Reden: Ik keur dit document goed  
Project leader:	De Maerschalck, B.	Getekend door: Bart De Maerschalck (Sig) Getekend op: 2024-09-17 17:12:12 +02:0 Reden: Ik keur dit document goed  

## Approval

Head of Division:	Bellafkih, K.	Getekend door: Abdelkarim Bellafkih (Sign) Getekend op: 2024-09-17 16:03:12 +02:0 Reden: Ik keur dit document goed  
-------------------	---------------	--

# Abstract

The presented report describes the efforts done to make the TELEMAC-MASCARET suite capable of simulating cross-shore sediment transport, which currently is not in the list of the model's capabilities, through the implementation of the different cross-shore processes in GAIA and TOMAWAC modules.

Prior to the implementation of the major cross-shore processes in the wave and sediment transport modules of TELEMAC, another well-known model for morphological simulations near the coast, XBeach, which incorporates the most important cross-shore process, is utilized for the reproduction of the results of a well known large scale laboratory experiment (CROSSTEX) for cross-shore transport over a mobile sandy bed.

The cross-shore processes that found to be of high importance through the XBeach validation, are implemented in GAIA and TOMAWAC modules. The validation of the updated modules is done again by comparison to the CROSSTEX laboratory measurements, considering both erosive and accretive conditions.

Taking into account the findings of the calibration/validation tests for both models, it is demonstrated that TELEMAC-2D – TOMAWAC – GAIA coupled model presents better behavior in reproducing cross-shore transport under both erosive and accretive conditions, compared to the XBeach model. Note that the comparison was based on the utilization of similar formulations for the considered processes by both models.

# Contents

Abstract .....	III
Contents .....	IV
List of tables.....	V
List of figures .....	VI
1 Introduction.....	1
2 CROSSTEX laboratory experiment.....	2
3 XBeach modelling .....	4
3.1 Offshore Bar Generation (OG) case .....	4
3.2 Middle Bar Generation (MG) case .....	9
4 GAIA modelling.....	14
4.1 Theoretical background .....	14
4.1.1 Advection-diffusion equation .....	14
4.1.2 Stokes drift – Return flow .....	15
4.1.3 Wave non-linearity .....	15
4.1.4 Surface rollers .....	15
4.1.5 Wave breaking turbulence .....	16
4.2 Offshore Sandbar Generation (OG) case .....	17
4.3 Middle Sandbar Generation (MG) case .....	24
5 Conclusions.....	30
References .....	31

## List of tables

Table 1: Wave conditions and duration of the two first phases of the CROSSTEX experiment.....	3
Table 2: Calibrated parameters of Janssen & Battjes wave breaking model (2007) for the OG case.....	4
Table 3: Xbeach parameters and processes investigated in sensitivity tests for the OG case.....	5
Table 4: Calibrated parameters of the (extended) Roelvink wave breaking model (1993) for the OG case. ....	8
Table 5: Calibrated parameters of Janssen & Battjes wave breaking model (2007) for the MG case.....	10
Table 6: Xbeach parameters and processes investigated in sensitivity tests for the MG case.....	11
Table 7: Calibrated parameters of Battjes & Janssen wave breaking model (1978) for the OG case.....	17
Table 8: GAIA, TOMAWAC & TELEMAC2D parameters and processes investigated in sensitivity tests for the OG case. ....	18
Table 9: Calibrated parameters of Battjes & Janssen wave breaking model (1978) for the MG case.....	24
Table 10: GAIA & TOMAWAC parameters and processes investigated in sensitivity tests for the MG case..	25

## List of figures

Figure 1: Initial bathymetry for the CROSSTEX experiment. ....	2
Figure 2: Measured initial and final bathymetries for the OG phase (top) and MG phase (bottom) during the CROSSTEX experiment. ....	3
Figure 3: Modelled by XBeach significant wave height variation at the breaking zone and the surf zone for the CROSSTEX experiment [OG case]. ....	5
Figure 4: Total bed level change at the end of the XBeach simulations for the runs of Table 3 [OG case]. ....	6
Figure 5: Measured and modelled bottom evolution at the end of the OG phase; top: Smagorinski model; bottom: constant viscosity. ....	7
Figure 6: Measured and modelled bottom evolution at the end of the OG phase for the run with deactivated wave non-linearity. ....	8
Figure 7: Total bed level change at the end of the simulation for the 1D (cstx83), Q2D (cstx91) and surfbeat (cstx92) runs [OG case]. ....	9
Figure 8: Modelled by XBeach significant wave height variation at the breaking zone and the surf zone for the CROSSTEX experiment [MG case]. ....	10
Figure 9: Measured and modelled bottom evolution at the end of the MG phase for the run cstxA23 (see Table 6). ....	11
Figure 10: Total bed level change at the end of the simulation for the runs of Table 6 [MG case]. ....	12
Figure 11: Measured and modelled bottom evolution at the end of the MG phase for the run cstxA30 (see Table 6). ....	13
Figure 12: Measured and modelled bottom evolution at the end of the MG phase for the surfbeat run (cstxA32). ....	13
Figure 13: Modelled by TOMAWAC significant wave height variation at the breaking zone and the surf zone for the CROSSTEX experiment [OG case]. ....	17
Figure 14: Measured and modelled bottom evolution at the end of the OG phase for the run with the optimal settings (ctx144). ....	19
Figure 15: Total bed level change at the end of the GAIA simulations for the runs of Table 8 [OG case]. ....	20
Figure 16: Measured and modelled bottom evolution at the end of the OG phase for the runs with different $R_{cs}$ values. ....	20
Figure 17: Measured and modelled bottom evolution at the end of the OG phase for the run with deactivated wave non-linearity. ....	21
Figure 18: Measured and modelled bottom evolution at the end of the OG phase for the run with only return flow activated. ....	21
Figure 19: Modelled bottom evolution at the end of the OG phase for the run with the Smagorinski model activated. ....	22
Figure 20: Measured (red circles) and modelled (blue lines) results for the run with the optimal settings (ctx144) for the OG case. ....	23
Figure 21: Modelled by TOMAWAC significant wave height variation at the breaking zone and the surf zone for the CROSSTEX experiment [MG case]. ....	24

Figure 22: Measured and modelled bottom evolution at the end of the MG phase for the runs ctxA047 & ctxA050 (see Table 10). .....	26
Figure 23: Measured and modelled bottom evolution at the end of the MG phase for the runs of wave non-linearity calibration.....	26
Figure 24: Measured and modelled bottom evolution at the end of the MG phase for the runs of concentration ratio $R_{cs}$ calibration. ....	27
Figure 25: Measured and modelled bottom evolution at the end of the MG phase for the runs of beta factor (surf roller) calibration.....	28
Figure 26: Measured and modelled bottom evolution at the end of the MG phase for the runs with deactivated wave turbulence (ctxA060) and deactivated surface rollers + wave turbulence (ctxA059). .....	28
Figure 27: Measured (red circles) and modelled (blue lines) results for the run with the optimal settings (ctxA056) for the MG case.....	29



# 1 Introduction

The last years TELEMAC open-source platform has present significant development in the wave-induced sediment transport modelling becoming a reliable tool for short- and long-term morphological simulations at the nearshore areas. The main reason behind this achievement is that a lot of physical processes related to the wave propagation and nearshore transformation, have already been implemented successfully in the code. However, there is still space for further development and for incorporation of additional important mechanisms that drive sediment transport. The work presented in the following chapters is an attempt to make TELEMAC suite capable of simulating cross-shore sediment transport, which currently is not in the list of the model's capabilities, through the implementation of the different cross-shore processes in GAIA and TOMAWAC modules.

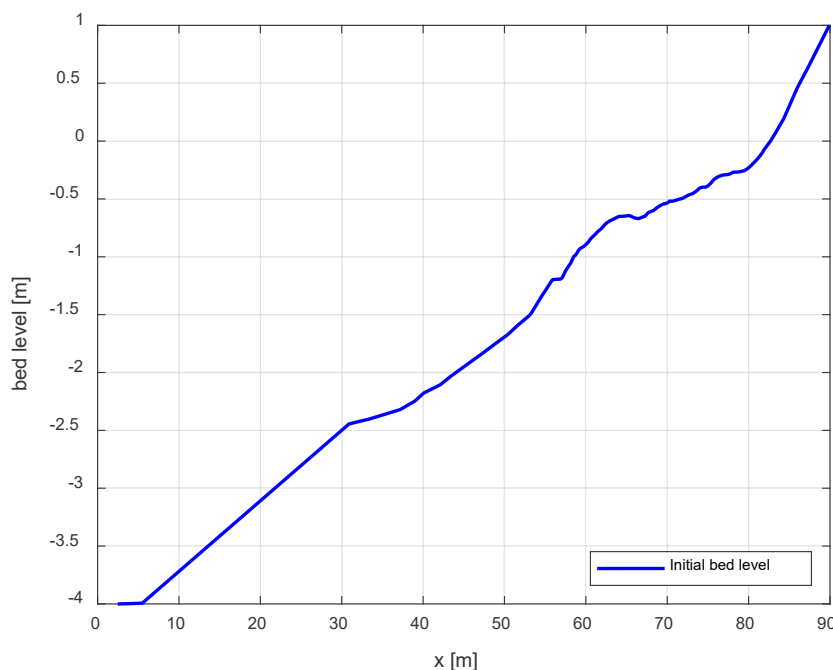
Prior to the implementation of the major cross-shore processes in the wave and sediment transport modules of TELEMAC, another well-known model for morphological simulations near the coast, XBeach, which incorporates the most important cross-shore process, is utilized for the reproduction of the results of a well known large scale laboratory experiment (CROSSTEX) for cross-shore transport over a mobile sandy bed. In this manner, the importance of each cross-shore process is evaluated, based on their contribution on sediment transport and bed morphology evolution, before implemented in the corresponding modules of TELEMAC platform. Note that the laboratory experiment was divided in phases that represented both storm (erosive) and mild (accretive) wave conditions.

Next, the cross-shore processes that found to be of high importance through the XBeach validation, are implemented in GAIA and TOMAWAC modules. The validation of the updated modules is done again by comparison to the CROSSTEX laboratory measurements, considering both erosive and accretive conditions.

In the following chapters, apart from the presentation of the results of the XBeach and GAIA validation, the main information about the CROSSTEX experiment (set-up, measured data) and the theoretical background of the considered mechanisms that contribute in cross-shore transport, are given.

## 2 CROSSTEX laboratory experiment

One of the available laboratory experiments for the investigation of cross-shore sediment transport processes over a mobile (sandy) bed, is the so-called 'CROSSTEX' experiment (Cobo et al., 2007; Guannel, 2009) that was conducted in the Large Wave Flume (LWF) facility at Oregon State University. The LWF is 104 meters long, 3.7 meters wide and 4.6 meters deep and the waves were generated by a flap-type wavemaker. The initial beach profile (FIGURE) combined the following characteristics: A bar was formed on an inclined beach of (average) slope 1:20, the foreshore slope and the surf zone slope was 1:7 and 1:17, respectively, while the offshore slope was 1:33. The bed was filled with fine to medium natural sand of  $d_{50}=0.2$  mm.



---

Figure 1: Initial bathymetry for the CROSSTEX experiment.

---

The experiment included wave forcing periods (runs) of 15 min each, during which, free surface elevation, flow velocity, sediment concentrations were measured at fixed locations. The bed level was also measured at the end of each run. The experiment was divided in 4 phases:

1. Offshore Bar Generation (OG)
2. Middle Bar Generation (MG)
3. Middle Bar Stagnation (MS)
4. Middle Bar Degeneration (MD)

In this report the two first phases are only taken into account (OG and MG). During the first phase (OG), relatively high energy waves were produced in order to simulate storm conditions (erosive case), while during the second phase (MG) fair-weather conditions were produced (accretive case). The main characteristics of the wave forcing for the aforementioned sets of runs are presented in Table 1. Note that the waves were irregular, generated by use of the TMA spectrum. The bathymetric changes observed at the end of the two investigated cases (OG and MG), are shown in Figure 2. During the OG phase the migration and the formation of a stronger bar to the offshore of the initial one is observed, while during the MG phase the the offshore bar vanished and a new one is formed at relatively shallower depth.

Table 1: Wave conditions and duration of the two first phases of the CROSSTEX experiment.

Experimental Phase	Run Intervals	Wave Height $H_s$ [m]	Peak Wave Period $T$ [s]	Spectral Peak factor $\gamma$	Duration [min]
Offshore Bar Generation (OG)	14	0.6	4.0	2	210
Middle Bar Generation (MG)	45	0.3	8.0	10	675

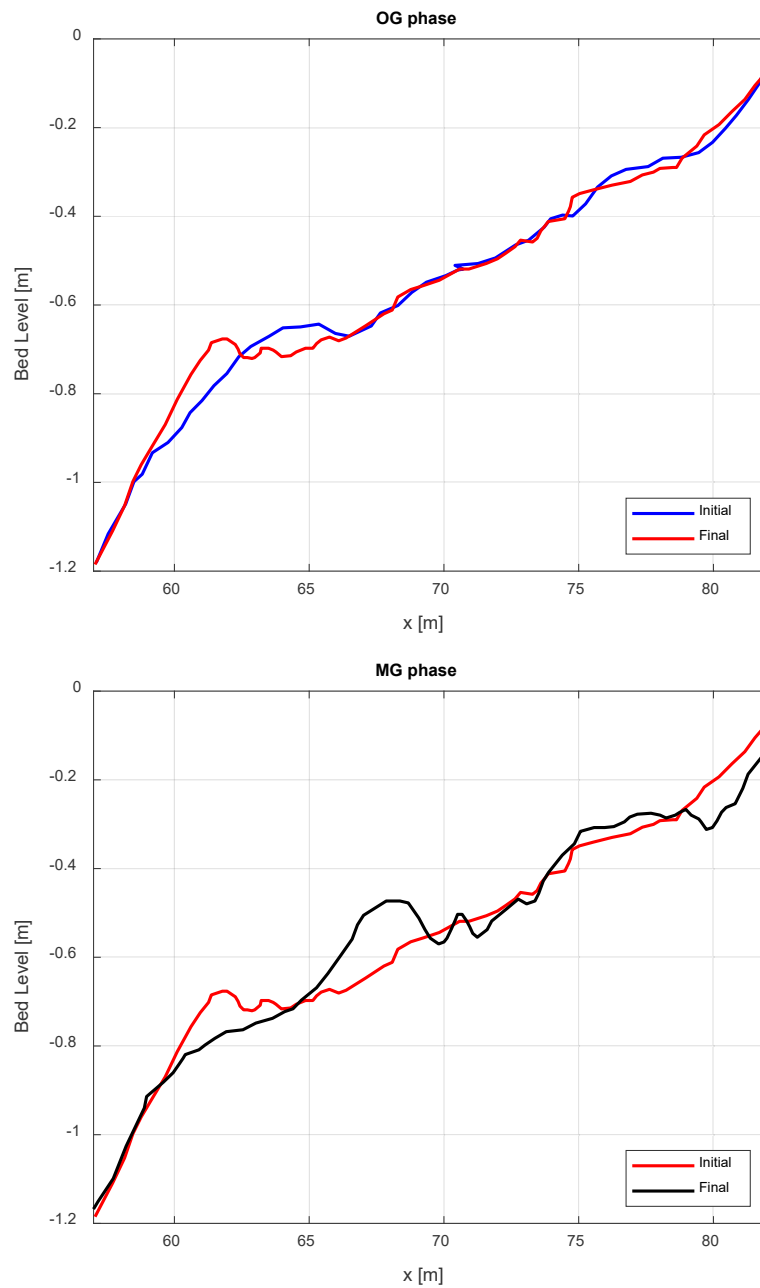


Figure 2: Measured initial and final bathymetries for the OG phase (top) and MG phase (bottom) during the CROSSTEX experiment.

## 3 XBeach modelling

Prior to the implementation of the different cross-shore processes in GAIA and TOMAWAC modules, XBeach model is utilized for the reproduction of the results of CROSSTEX laboratory experiment. In this manner, the importance of each cross-shore process is evaluated, based on their contribution on sediment transport and bed morphology evolution, before implemented in the corresponding modules of TELEMAC platform. To this end, numerical simulations of the two phases, i.e. the erosive (OG) and the accretive (MG) case, are performed and the results are presented in the following sections. An one-dimensional computational domain of length equal to 90 m has been considered and the mesh resolution was set to 0.2 m. A varying time-step was considered, which resulted by the satisfaction of the CFL criterion ( $< 0.9$ ), applied constantly during the computation. It is noted that the stationary mode of XBeach, which takes into account only short waves, is utilized in the simulations presented in this report. Indicative runs per case (OG and MG) with surfbeat (instationary) mode, are performed for comparison.

The utilized XBeach version was *v1.23.5917-BOI-candidate* installed in WL cluster. This version was recompiled due to a bug in subroutine *wave\_stationary\_directions.F90*, which led to zero wave orbital velocities  $U_{orb}$ .

### 3.1 Offshore Bar Generation (OG) case

As wave breaking is the most important mechanism that drives cross-shore sediment transport, especially in storm conditions, wave breaking calibration takes place first (prior to the morphological simulations), considering a non-movable bottom. The utilized wave breaking model is the one proposed by Janssen & Battjes, (2007), which is suitable for stationary waves and it is a revision of the Baldock's model (Baldock et al., 1998). The values of the basic tuning parameters of Janssen & Battjes model (JB07), before and after calibration, are shown in Table 2. The cross-shore variation of significant wave height ( $H_s$ ) for both versions of the JB07 model against the measurements are shown in Figure 3. Note that the *gammax* parameter, which determines the maximum ratio of wave height to water depth, affects wave height only very close to the shoreline, resulting into local the bed level change.

Table 2: Calibrated parameters of Janssen & Battjes wave breaking model (2007) for the OG case.

JB07 parameters	default	calibrated
<i>gamma</i>	0.78	<b>0.55</b>
<i>alpha</i>	1.38	<b>0.9</b>
<i>gammax</i>	0.6	0.6

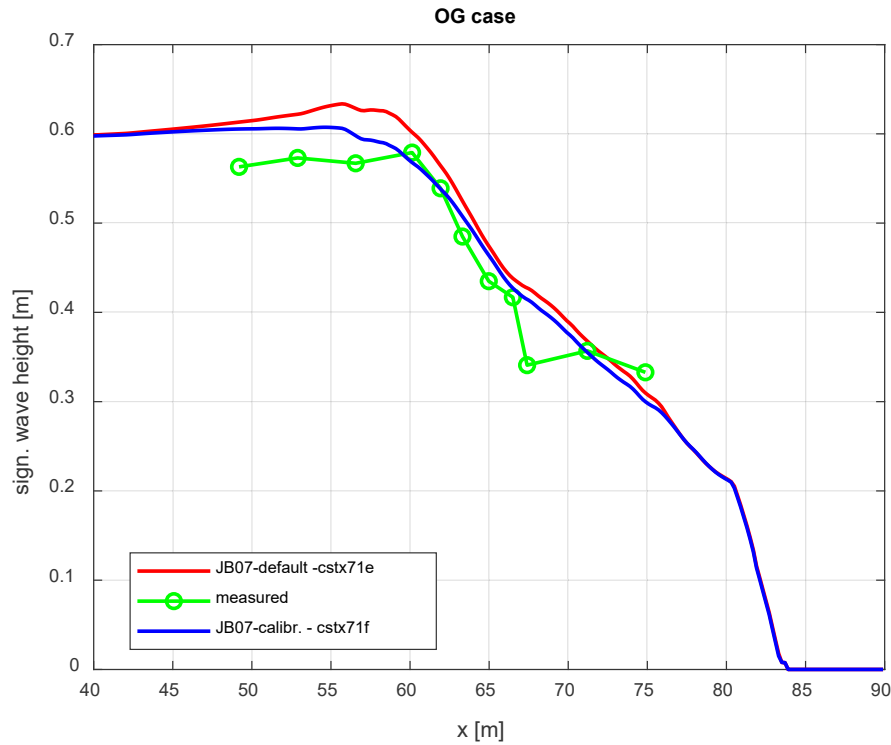


Figure 3: Modelled by XBeach significant wave height variation at the breaking zone and the surf zone for the CROSSTEX experiment [OG case].

Then, a series of sensitivity tests (runs) for the main mechanisms that drive cross-shore sediment transport was performed considering movable bed and simulation period equal to the duration of the OG phase. The parameters of the morphological simulations are summarized in Table 3.

Table 3: Xbeach parameters and processes investigated in sensitivity tests for the OG case.

Run	Tuned parameter	XBeach parameter			
		Roller/beta	Turbulence	$f_{AS} / f_{SK}$	<i>Smag. model</i>
<b>cstx82</b>	none/default values	YES / 0.1	Wave averaged	0.1 / 0.1	YES
<b>cstx83</b>	surface roller-beta	YES / <b>0.07</b>	Wave averaged	0.1 / 0.1	YES
<b>cstx85</b>	asymmetry-skewness	YES / 0.07	Wave averaged	<b>0.1 / 0.3</b>	YES
<b>cstx86</b>	asymmetry-skewness	YES / 0.07	Wave averaged	<b>0.0 / 0.0</b>	YES
<b>cstx87</b>	wave turbulence	YES / 0.07	<b>None</b>	0.1 / 0.1	YES
<b>cstx88</b>	roller- w. turbulence	<b>NO / -</b>	<b>None</b>	0.1 / 0.1	YES
<b>cstx89</b>	roller-turb.-nonlinearity	<b>NO / -</b>	<b>None</b>	<b>0.0 / 0.0</b>	YES
<b>cstx90</b>	subgrid turb. model	YES / 0.07	Wave averaged	0.1 / 0.1	<b>NO</b>

Apart from the Stokes drift and the (coupled) return flow, which is responsible for the offshore-directed sediment transport, one of the main mechanisms contributing substantially to the cross-shore sediment transport is the development of a surface roller in the breaking wavefront. Surface rollers are included in XBeach model and they contribute to the mean cross-shore current by means of an extra velocity component which is offshore directed. The contribution of surface rollers can be adjusted by the breaker slope coefficient  $\beta$ .

The wave non-linearity, which consists of two components, i.e. wave asymmetry and skewness, contributes to the mean cross-shore current as an extra velocity component which is onshore directed. The influence of wave non-linearity can be adjusted by two calibration factors, i.e.  $f_{As}$  for the wave asymmetry and  $f_{Sk}$  for the wave skewness.

Another important mechanism for stirring up sediment, is the wave breaking turbulence, which is directly related to the development of surface rollers. Apparently near bed turbulence is not taken into account by the model, if surface rollers are excluded from the simulation.

In Figure 4, the total bed level change at the end of the simulation period of OG phase for the runs included in Table 3, is presented. The main findings are:

- Decreasing breaker slope coefficient  $\beta$  enhances the offshore bar formation.
- Increased wave non-linearity (through skewness calibration factor) decelerates the bar migration to the offshore direction.
- Omitting wave non-linearity allows bar to move offshore much easier.
- The impact of wave breaking turbulence is important for the bar migration to the offshore.
- Minor bed level changes occur when rollers are deactivated and wave non-linearity is activated.
- Return flow by itself (surface rollers, turbulence and wave non-linearity deactivated) has limited impact on the bar migration to the offshore.

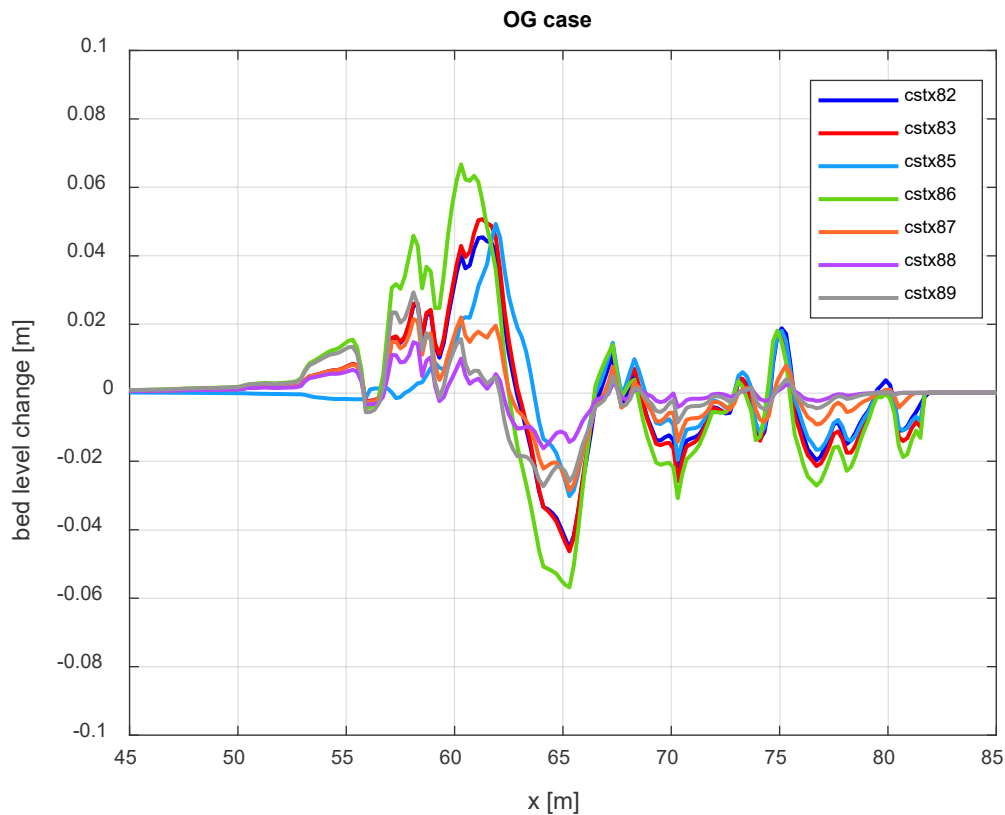


Figure 4: Total bed level change at the end of the XBeach simulations for the runs of Table 3 [OG case].

The modelled bed evolution for the optimal XBeach settings, against the measured bed level at the end of OG phase, is shown at the top panel of Figure 5. In general, the model is capable of predicting the offshore bar migration fairly good. However the height of the bar in the simulation is substantially smaller than the measured one. In the bottom panel of Figure 5, the impact of considering constant horizontal viscosity ( $\nu_{uh} = 0.1 \text{ m}^2/\text{s}$ ) instead of the Smagorinski model (default option), on the bed evolution, is shown. Obviously, the Smagorinski model helps the eroded sediment of the initial bar to form another offshore bar, while constant viscosity indicates a clear diffusive behavior.

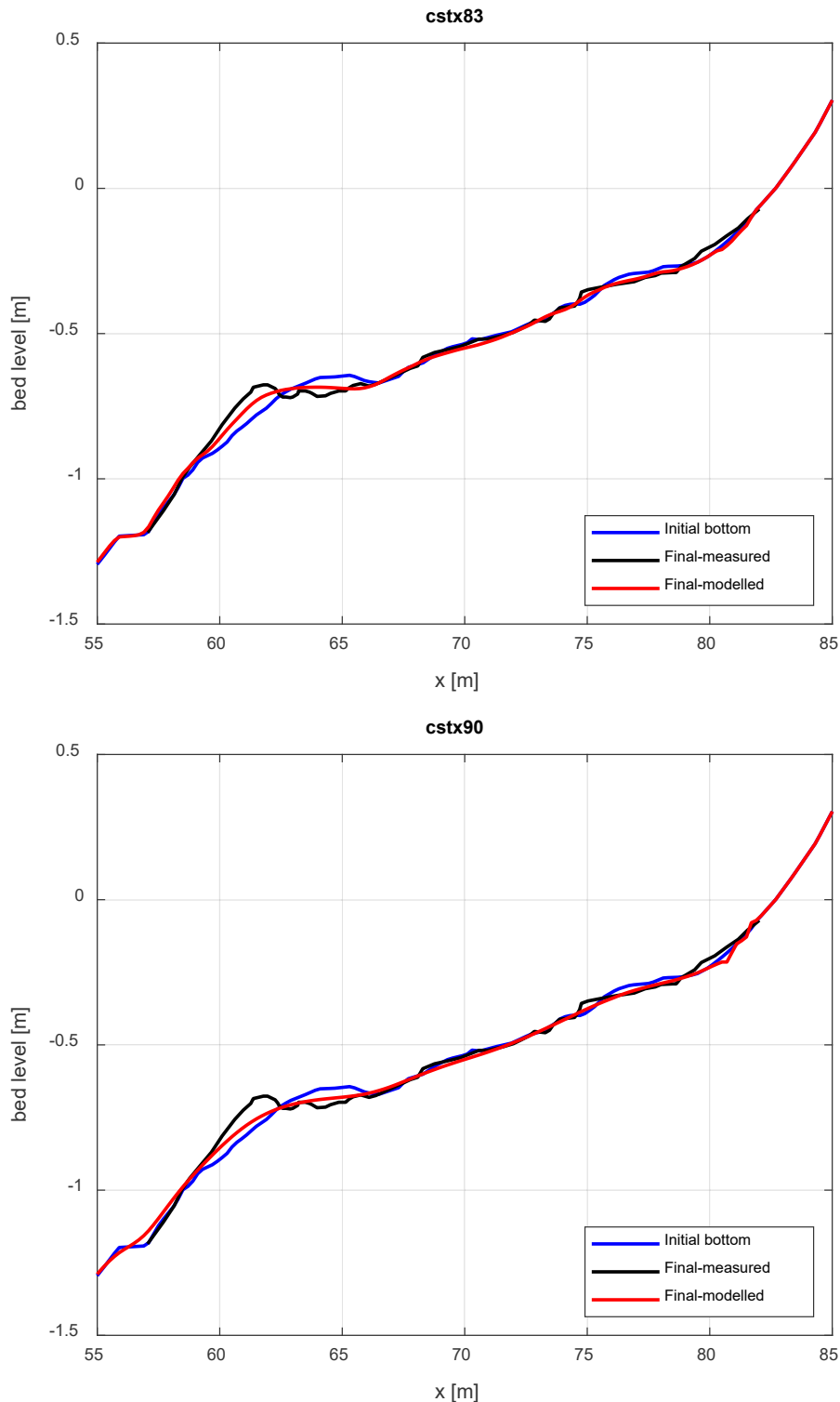


Figure 5: Measured and modelled bottom evolution at the end of the OG phase; top: Smagorinski model; bottom: constant viscosity.

The bottom level at the end of the simulation period for the case of deactivated wave non-linearity is compared to the measured one at the end of the OG phase (Figure 6). It seems that the model predicts accurately the erosion of the initial bar and fairly good the deposition to the offshore. This result indicates that wave-nonlinearity impact should be rather limited in case of storm (erosive) conditions.

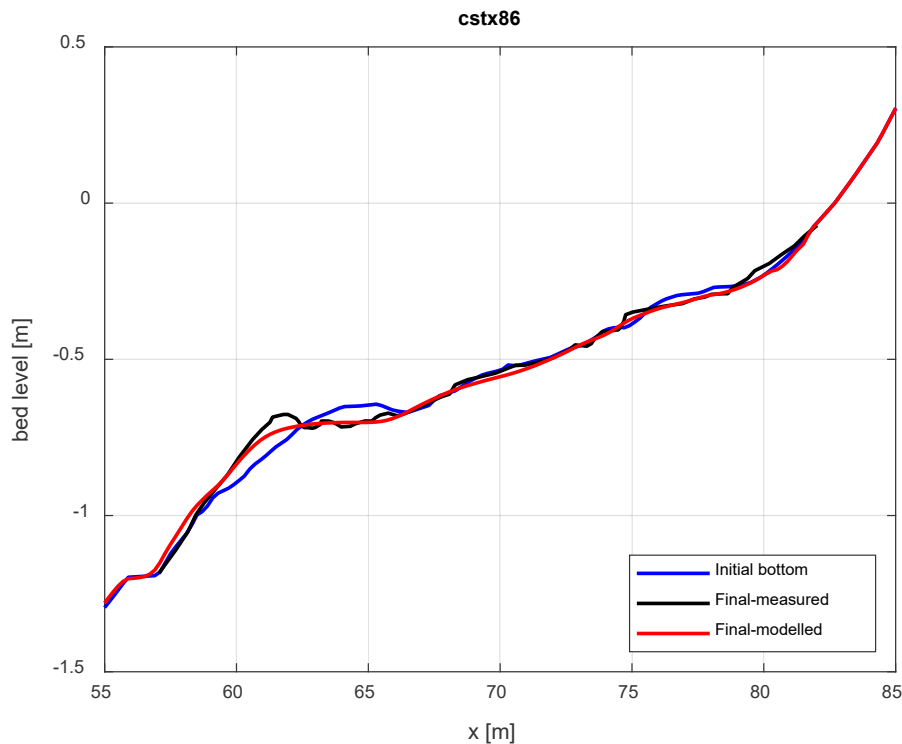


Figure 6: Measured and modelled bottom evolution at the end of the OG phase for the run with deactivated wave non-linearity.

Additionally, two modelling tests were performed for the OG case and that is:

- The consideration of two-dimensional (2DH) computational domain with uniform bed level in the transverse (y-)direction (cstx91). Ten (10) computational cells were considered in the y-direction and the resolution remained the same as in x-direction, equal to 0.2 m.
- The activation of long waves by selecting the surfbeat (instationary) module of XBeach (cstx92). For this simulation wave breaking calibration had to be repeated, as the JB07 model used in the stationary runs doesn't apply for surfbeat mode. The extended model by Roelvink (1993) was calibrated, and the optimal for the case parameters are shown in Table 4.

Table 4: Calibrated parameters of the (extended) Roelvink wave breaking model (1993) for the OG case.

roelvink2 parameters	default	calibrated
gamma	0.55	<b>0.45</b>
alpha	1.0	<b>1.3</b>
gammax	2.0	<b>0.6</b>



In Figure 7, the total bed level change at the end of the simulation period of OG for the Quasi-2D (cstx91) and the surfbeat (cstx92) runs, is presented. For comparison, the results by the 1D stationary run with the optimal settings (cstx83) are also shown. Note that the parameters for the Quasi-2D run are identical to the reference run (cstx83), while for the case of the surfbeat run, only the breaking parameters are different. Obviously, the results of the 1D and the Quasi-2D model are almost identical. Noticeable differences are located very close to the shoreline. As for the surfbeat run, the comparison shows a general agreement with the reference run at the breaking and surf zone, but larger differences at the swash zone.

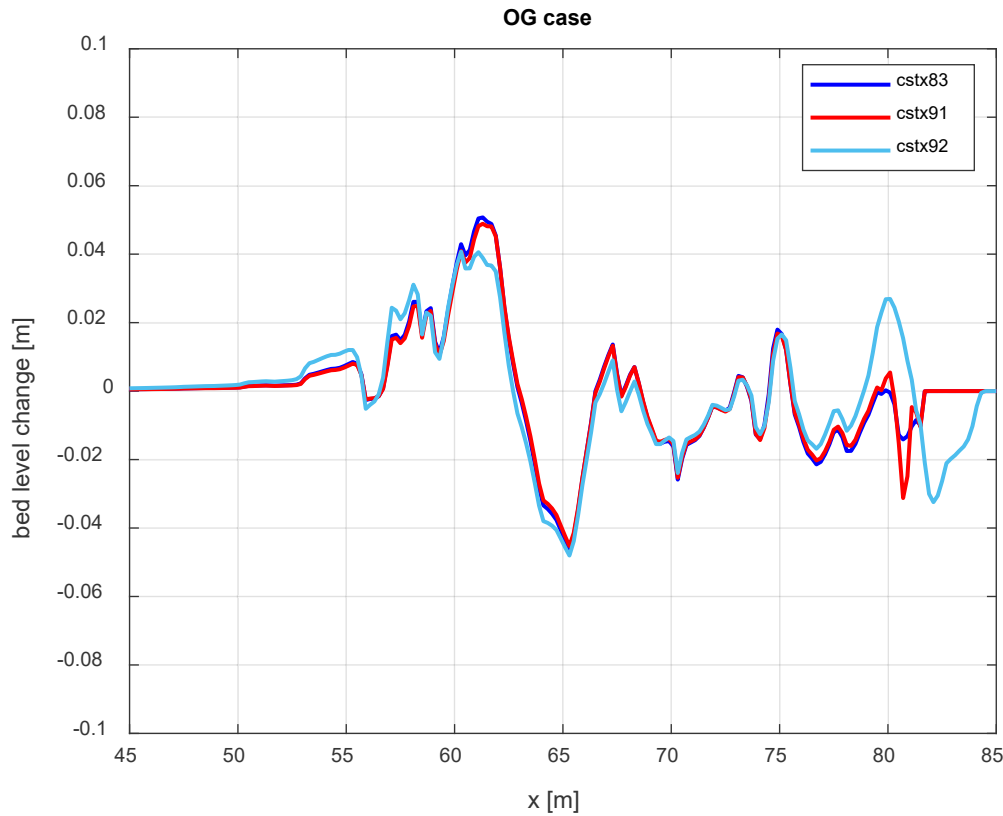


Figure 7: Total bed level change at the end of the simulation for the 1D (cstx83), Q2D (cstx91) and surfbeat (cstx92) runs [OG case].

### 3.2 Middle Bar Generation (MG) case

Wave breaking calibration needs to take place first also for the MG case, which corresponds to milder wave conditions (accretive), as XBeach model is mainly designed to simulate storm events. As in the OG case, during the wave breaking calibration the bottom is considered as frozen and the utilized wave breaking model is the one proposed by Janssen & Battjes, (2007). The values of the basic tuning parameters of Janssen & Battjes model (JB07), before and after calibration, are shown in Table 5. The cross-shore variation of significant wave height ( $H_s$ ) for both versions of the JB07 model against the measurements are shown in Figure 8. Note that the intensity of wave breaking in MG case is relatively low, compared to the one of the OG case, hence this process is less sensitive to the adjustment of the calibration parameters. However, it seems that wave height dissipation in the inner surf zone/swash zone is quite sensitive to the *gamma*max parameter, resulting in sensitivity of the bed level changes. Note that the *gamma* and the *alpha* parameters take the same values for both OG (erosive) and MG (accretive) cases.

Table 5: Calibrated parameters of Janssen & Battjes wave breaking model (2007) for the MG case.

JB07 parameters	default	calibrated
gamma	0.78	<b>0.55</b>
alpha	1.38	<b>0.9</b>
gammax	0.6	<b>1.0</b>

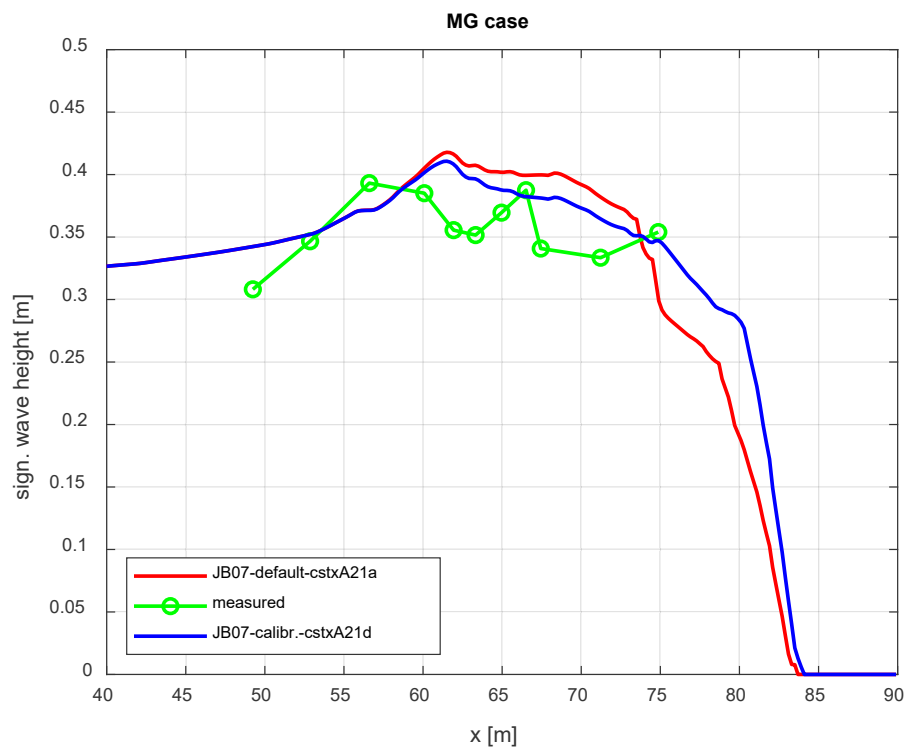


Figure 8: Modelled by XBeach significant wave height variation at the breaking zone and the surf zone for the CROSSTEX experiment [MG case].

Then, a series of sensitivity tests (runs) for the main mechanisms that drive cross-shore sediment transport was performed considering movable bed and simulation period equal to the duration of the MG phase. The parameters of the morphological simulations are summarized in Table 6. The investigated parameters are: the *gammax* factor (wave breaking), the *beta* parameter (surface rollers), the asymmetry and skewness parameters (wave non-linearity). Finally, a test with deactivated surface rollers and wave breaking turbulence is performed.

In Figure 9, the modelled bed evolution for the calibrated wave breaking model (Table 5) and the optimal XBeach settings from the OG case (run cstx83), is presented against the measured bed level at the end of MG phase, in order to get a general view of the model's performance in accretive conditions. The main finding is that the model fails to predict the middle bar generation, as the offshore bar keeps more or less its initial position. The model predicts rather overestimated erosion close to the shoreline, where the bed slope becomes quite abrupt. The eroded sediment seems to be accumulated between  $x=71$  m and  $x=75$  m.

Table 6: Xbeach parameters and processes investigated in sensitivity tests for the MG case.

Run	Tuned parameter	XBeach parameter			
		<i>gammax</i>	Roller/beta	Turbulence	$f_{AS} / f_{SK}$
<b>cstxA22</b>	settings identical to cstx83	0.6	YES / 0.07	Wave averaged	0.1 / 0.1
<b>cstxA23</b>	wave breaking- <i>gammax</i>	<b>1.0</b>	YES / 0.07	Wave averaged	0.1 / 0.1
<b>cstxA24</b>	surface roller-beta	1.0	YES / <b>0.15</b>	Wave averaged	0.1 / 0.1
<b>cstxA30</b>	asymmetry-skewness	1.0	YES / 0.07	Wave averaged	<b>0.5 / 0.5</b>
<b>cstxA31</b>	roller-w. turbulence	1.0	<b>NO / -</b>	<b>None</b>	0.5 / 0.5

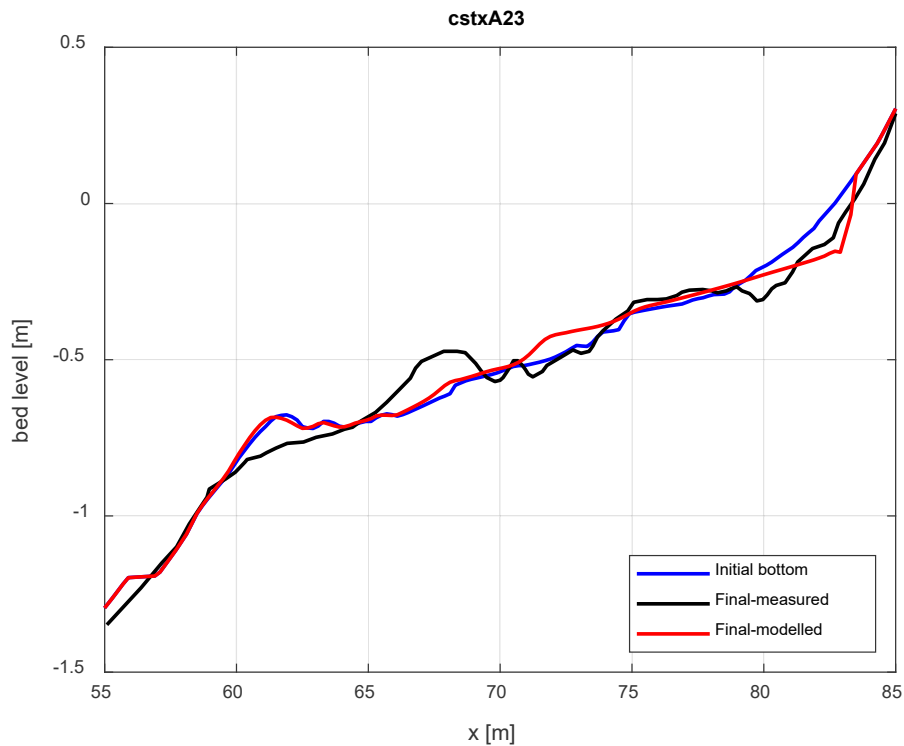


Figure 9: Measured and modelled bottom evolution at the end of the MG phase for the run cstxA23 (see Table 6).

In Figure 10, the total bed level change at the end of the simulation period of MG phase for the runs included in Table 6, is presented. The main findings are:

- Increasing *gammax* factor, which stands for the maximum ratio of wave height to water depth, results into substantial sedimentation/erosion only for (shallow) depths lower than 0.5 m (for  $x > 70$  m).
- Increasing breaker slope coefficient *beta* doesn't affect the migration of the offshore bar. At shallow water depths results into relatively less sedimentation/erosion.

- Increased wave non-linearity (through asymmetry and skewness calibration factors) triggers the onshore migration of the offshore sandbar and substantially reduces the erosion at shallow depths ( $x > 80$  m). However, increased sedimentation is observed at  $75 \text{ m} < x < 80 \text{ m}$ .
- The deactivation of the mechanisms that contribute to the offshore directed transport, i.e. surface rollers and wave breaking turbulence, coupled with the enforcement of wave non-linearity, result into an accretive behavior at the shallower depths ( $x > 75 \text{ m}$ ). On the other hand, it seems that the onshore migration of the offshore sandbar is not affected by the deactivated mechanisms.

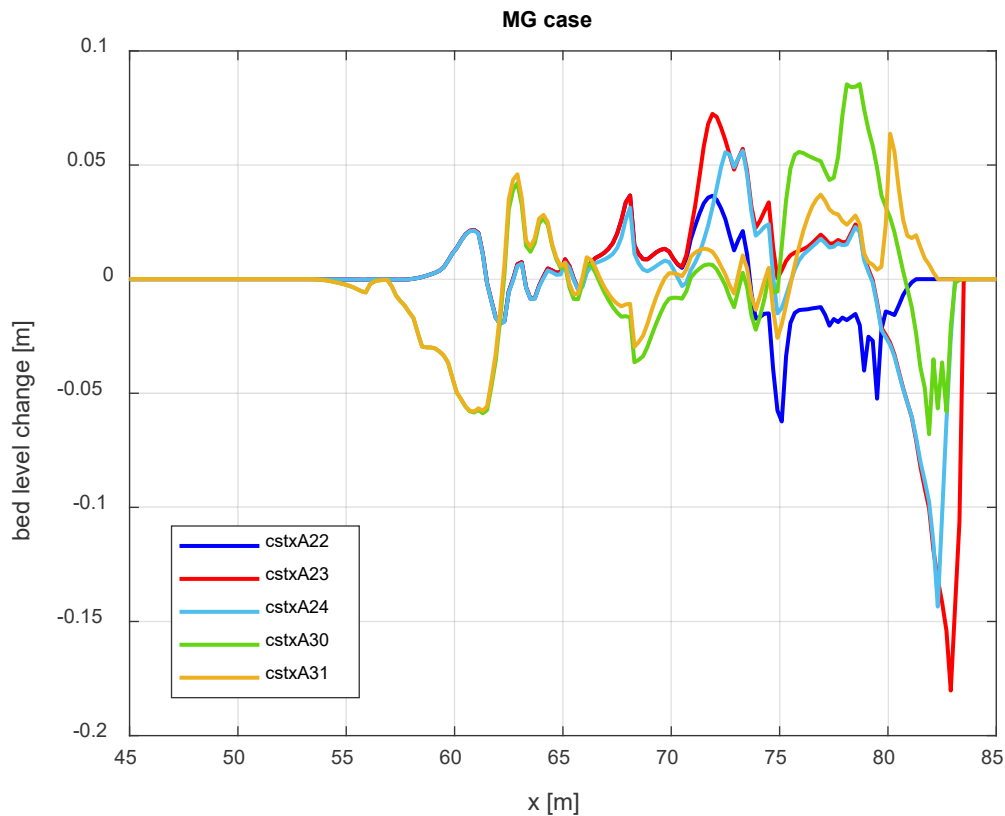


Figure 10: Total bed level change at the end of the simulation for the runs of Table 6 [MG case].

In Figure 11, the modelled bed evolution for the run with the enforced wave non-linearity (cstxA30), is presented against the measured bed level at the end of MG phase. It seems that the model finds it difficult to predict the middle sandbar generation, however a onshore migration of the offshore sandbar can be noticed. The model underestimates the measured erosion at shallow depths ( $< 0.3 \text{ m}$ ), obviously due to the enhanced action of wave-non linearity, which apparently dominates over the mechanisms that cause offshore directed transport (surface rollers, turbulence).

The simulation with the increased wave-nonlinearity (cstxA30) was repeated by means of the surfbeat (instationary) module of XBeach (run cstxA32). For this simulation wave breaking calibration had to be repeated, as the JB07 model used in the stationary runs doesn't apply for surfbeat mode. The extended model by Roelvink (1993) was calibrated, and the optimal for the case parameters were:  $\gamma = 0.35$ ,  $\alpha = 1.1$  and  $\gamma_{\max} = 1.0$ . Figure 12 shows the modelled bed evolution for the this run against the measured bed level at the end of MG phase. It seems that the surfbeat mode gives similar results with the corresponding stationary one (Figure 11), with minor differences found at the shallow water (for  $x > 75 \text{ m}$ ).

Overall, the XBeach model seems to be insufficient for morphological simulations under mild (accretive) wave conditions.

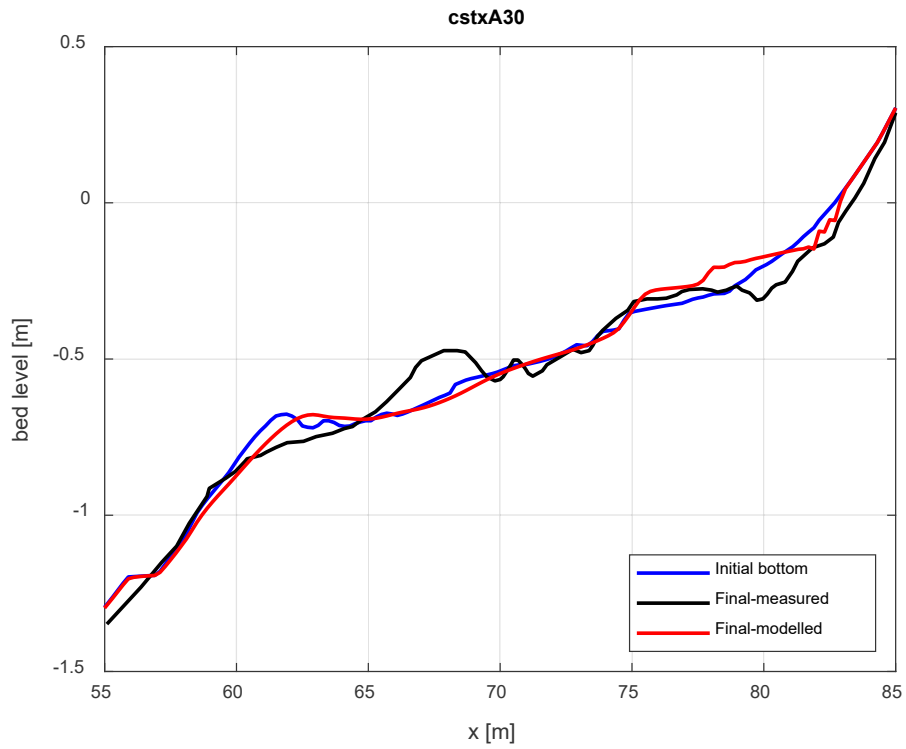


Figure 11: Measured and modelled bottom evolution at the end of the MG phase for the run cstxA30 (see Table 6).

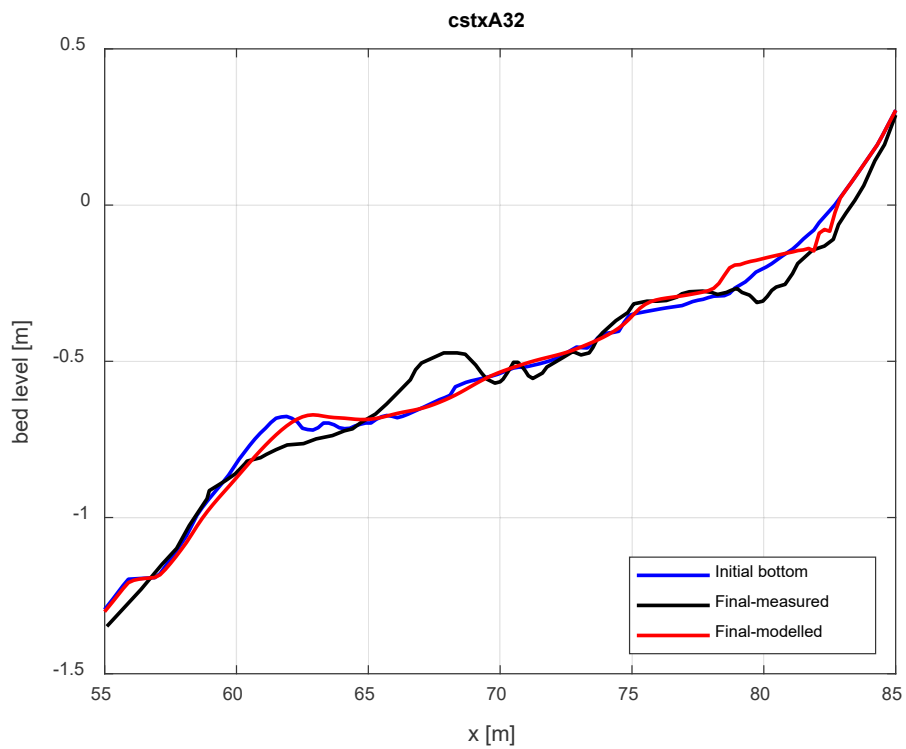


Figure 12: Measured and modelled bottom evolution at the end of the MG phase for the surfbeat run (cstxA32).

## 4 GAIA modelling

Next, the implementation of the cross-shore processes that found to be of high importance through the XBeach validation (presented in the previous chapter), takes place in GAIA and TOMAWAC modules. The validation of the updated models is done by comparison to the CROSSTEX laboratory measurements, for both the erosive (OG) and the accretive (MG) phases of the experiment. A two-dimensional computational domain (numerical flume) of length equal to 90 m and of width equal to 2m has been constructed, considering a rectangular (channel) grid with resolution set to 0.2 m in both directions. A sensitivity analysis for the selection of the time-step ( $dt$ ) of the computations showed that the results presented an acceptable independency for a value (less or) equal to  $d = 0.2$  s. Before presenting the results of the calibration/validation of the model, the theoretical background of how the implemented mechanisms contribute in cross-shore sediment transport is given. Note that the numerical results presented in this chapter, correspond to a cross-section in the middle of the transverse direction of the computational domain.

The utilized TELEMAC branch in this report is named '*scaldisCoast*' (commit 03429103) and it is installed in WL cluster. For the needs of the specific validation exercise, the modification of three subroutines was necessary. Specifically:

- *speini.f*: introduction of unidirectional waves only
- *con4wd.f*: deactivation of refraction
- *iniphy.f*: modification of the Jacobian for the spectral transformation
- *gaia\_cross\_shore.f*: introduction of the new transport mechanisms

A modification to subroutine *suspension\_sandflow\_gaia.f*, which is used for the calculation of the equilibrium concentration,  $C_{eq}$ , according to Soulsby-Van Rijn equation, took place in order to include the bed load component in the corresponding equation. This modification may be proposed as an update of the source code.

### 4.1 Theoretical background

#### 4.1.1 Advection-diffusion equation

The main cross-shore processes are incorporated in the sediment transport module through the mean velocities ( $U^E, V^E$ ) that are introduced in the depth-averaged advection-diffusion equation for the calculation of sediment mean concentration  $C$  in the water column:

$$\frac{\partial hC}{\partial t} + \frac{\partial hU^E C}{\partial x} + \frac{\partial hV^E C}{\partial y} + \frac{\partial}{\partial x} \left( h\varepsilon_s \frac{\partial C}{\partial x} \right) + \frac{\partial}{\partial y} \left( h\varepsilon_s \frac{\partial C}{\partial y} \right) = w_s (C_{eq} - C) R_{cs} \quad (1)$$

where  $t$  is time,  $x$  and  $y$  are the two horizontal dimensions of the numerical domain,  $h$  is the water depth,  $\varepsilon_s$  is the eddy viscosity,  $w_s$  is the settling velocity,  $C_{eq}$  the equilibrium concentration, and  $R_{cs}$  is the ratio between near-bed concentration and the mean concentration.

The (Eulerian) velocities  $U^E$  and  $V^E$  replace the mean velocities  $U^L$  and  $V^L$  (Lagrangian), which are calculated by the flow module (TELEMAC). The incorporation of the contribution of each cross-shore mechanism to the velocity field responsible for the advection of sediment can be expressed as:

$$\vec{U}^E = \vec{U}^L + (\vec{U}_{NL} - \vec{U}_{ST} - \vec{U}_{SR}) \quad (2)$$

where  $\vec{U}_{NL}$  is the contribution of wave non-linearity,  $\vec{U}_{ST}$  is the Stokes drift and  $\vec{U}_{SR}$  is the contribution of surface rollers. The aforementioned mechanisms are described in the following paragraphs.

#### 4.1.2 Stokes drift – Return flow

When waves approach the coastal areas, a mean current directed to the shore, called Stokes drift, is formed in the upper part of the water column, because the motion of water particles do not demonstrate a perfectly circular track. According to the Eulerian approach, this mean current has to be counterbalanced, hence an opposite directed current of the same magnitude, is developed in the water column below the wave trough, contributing to the offshore directed sediment transport. The Stokes drift is given by the following expression:

$$U_{ST} = E_w / \rho h c \quad (3)$$

where,  $E^w$  is the wave-group varying short wave energy given by the following expression:

$$E^w = \rho g H_s^2 / 16 \quad (4)$$

In the above expression  $\rho$  is the water density,  $c$  is the phase velocity,  $g$  is the gravitational acceleration and  $H_s$  is the significant wave height.

#### 4.1.3 Wave non-linearity

The wave non-linearity consists of two mechanisms, i.e. wave skewness and wave asymmetry, which both contribute to the onshore directed sediment transport.

Wave skewness ( $Sk$ ) indicates that wave crests are higher and shorter in duration than the troughs. The shoreward velocity under the crest is higher than the seaward velocity under the wave trough (skewness). Wave asymmetry ( $As$ ) refers to the higher acceleration of the wave front compared to the wave tail.

The contribution of wave non-linearity is calculated by means of an extra velocity component in the advection-diffusion equation:

$$U_{NL} = (f_{Sk}Sk - f_{As}As)u_{rms} \quad (5)$$

where  $f_{Sk}$  and  $f_{As}$  are calibration factors with values from 0 to 1.0 and a recommended value of 0.1,  $u_{rms}$  is the root-mean square wave orbital velocity computed as:

$$u_{rms} = U_w / \sqrt{2} \quad (6)$$

and  $U_w$  is the wave orbital velocity. The expressions for skewness  $Sk$  and asymmetry  $As$  can be found in (Fonias et al., 2021).

#### 4.1.4 Surface rollers

During wave breaking, part of the wave energy is transformed into momentum transferred in an aerated region at the wave front, known as the surface roller. The stored by the surface roller energy from the breaker is released in the surf zone contributing to the wave-induced sediment transport (offshore directed). The surface roller energy ( $E_r$ ) evolution and dissipation is given by the following energy balance equation (Ruessink et al., 2001):

$$\frac{d}{dx}(2E_r c \cos \theta) = -D_r + D_{br} \quad (7)$$

where  $D_{br}$  is the dissipation due to wave breaking,  $\vartheta$  is the mean wave angle and  $D_r$  is the roller dissipation given by:

$$D_r = 2g(\beta_s/\beta_2)E_r/c \quad (8)$$

where  $\beta_s$  and  $\beta_2$  are calibration parameters usually assumed equal to 0.1 and 1.0, respectively.

The contribution of surface rollers in cross-shore sediment transport is introduced by an extra velocity component in the advection-diffusion equation (Svendsen, 1984a):

$$U_{SR} = 2E_r/(ch) \quad (9)$$

#### 4.1.5 Wave breaking turbulence

Wave breaking is a process highly connected with the generation of turbulence is the collapsing wave front. In the surf zone turbulence energy is transferred towards the seabed resulting into stirring up of sediment. The model utilized for describing the wave-breaking turbulence impact near bed is proposed by van Thiel de Vries (2009) and it is based on the exponential decay model by Roelvink & Stive (1989). The model for the computation of the wave-averaged near-bed turbulence energy ( $k_b$ ) by van Thiel de Vries, adopted in the present work, is given by:

$$k_b = D_r^{2/3}/(\exp(h/L_{mix}) - 1) \quad (10)$$

where  $L_{mix}$  is the mixing length, expressed as the thickness of the surface roller and depends on the roller volume  $A_r$  (Svendsen, 1984b):

$$L_{mix} = \sqrt{A_r} = \sqrt{2E_r T/c} \quad (11)$$

where  $T$  is wave period.

Wave turbulence effect on sediment transport is introduced through the equilibrium concentration formula,  $C_{eq}$ , according to the suggestion by van Thiel de Vries (2009). Specifically, the Soulsby-van Rijn equation (Soulsby, 1997) is properly modified considering increased wave orbital velocity ( $U_w$ ) due to the contribution of turbulence:

$$C_{eq} = \frac{A_s}{h} \left( \sqrt{\bar{U}^2 + 0,018u_{rms,2}/C_d} - \bar{U}_{cr} \right)^{2.4} \quad (12)$$

where  $A_s$  is a coefficient that includes both bed load and suspended load parameters ( $A_{sb}$ ,  $A_{ss}$ ),  $\bar{U}$  is the mean current velocity,  $\bar{U}_{cr}$  is the critical velocity for the initiation of motion,  $C_d$  is the drag coefficient and  $u_{rms,2}$  is the modified root-mean-square wave orbital velocity:

$$u_{rms,2} = (\sqrt{U_w^2 + \gamma_{turb}k_b})/\sqrt{2} \quad (13)$$

where  $\gamma_{turb}$  is a turbulence coefficient which can be set equal to 1.45 according to by van Thiel de Vries (2009).



## 4.2 Offshore Sandbar Generation (OG) case

As in the case of XBeach validation, wave breaking calibration takes place first (prior to the morphological simulations), considering a non-movable bottom. The utilized wave breaking model is the one proposed by Battjes & Janssen (1978), which is the default option in TOMAWAC and it is based on the analogy of depth-induced breaking to the hydraulic jump. The values of the basic tuning parameters of Battjes & Janssen model (JB78), before and after calibration, are shown in Table 7. Note that two methods can be used for the computation of the maximum wave height  $H_m$ : method 1 is a simple relation to the water depth with one tuning parameter (GAMMA1) and method 2 is a more complex one, which involves the water depth, the wave characteristics and two tuning parameters (GAMMA1, GAMMA2). Finally, there is also a calibration parameter for the wave dissipation (ALPHA). The cross-shore variation of significant wave height ( $H_s$ ) for both versions of the JB78 model against the measurements are shown in Figure 13.

Table 7: Calibrated parameters of Battjes & Janssen wave breaking model (1978) for the OG case.

JB78 parameters	default	calibrated
$H_m$ COMPUTATION METHOD	1	2
BREAKING BJ COEFFICIENT GAMMA1	0.88	<b>0.80</b>
BREAKING BJ COEFFICIENT GAMMA2	0.80	0.80
BREAKING BJ COEFFICIENT ALPHA	1.00	<b>0.80</b>

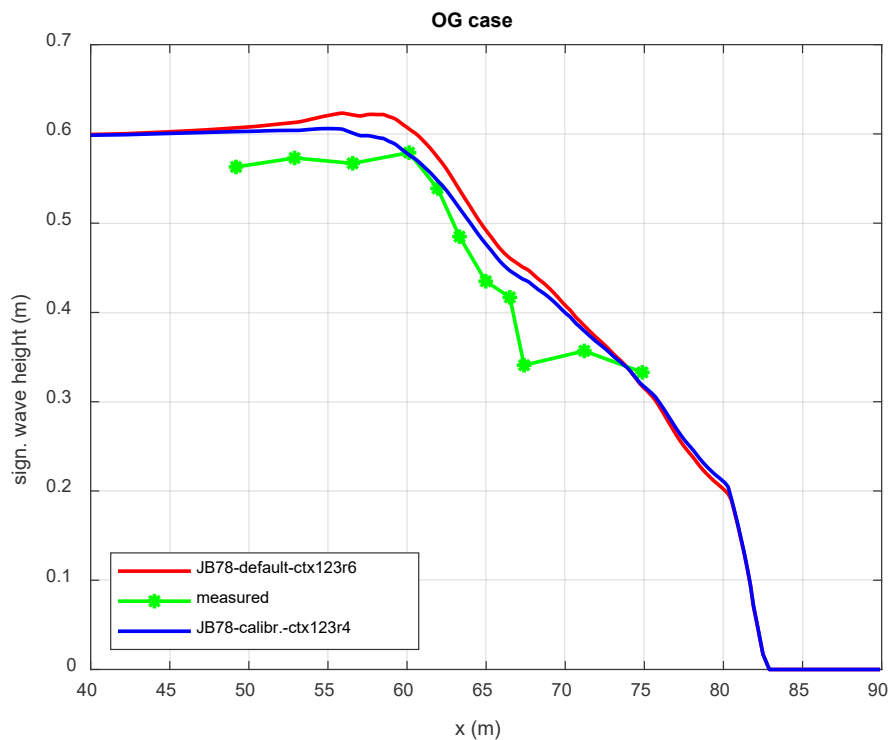


Figure 13: Modelled by TOMAWAC significant wave height variation at the breaking zone and the surf zone for the CROSSEX experiment [OG case].

Then, a series of sensitivity tests (runs) for the main mechanisms that drive cross-shore sediment transport was performed considering movable bed and simulation period equal to the duration of the OG phase. The parameters of the morphological simulations are summarized in Table 8.

Table 8: GAIA, TOMAWAC & TELEMAC2D parameters and processes investigated in sensitivity tests for the OG case.

Run	Tuned parameter	GAIA-TOMAWAC-T2D parameter				
		Roller/beta	Wave turbulence	$f_{AS} / f_{SK}$	$R_{cs}$	Flow turbulence
<b>ctx167</b>	none/default values	YES / 0.1	Wave averaged	0.1 / 0.1	1	Constant/ $v_t=0.1$
<b>ctx165</b>	concentration ratio $R_{cs}$	YES / 0.1	Wave averaged	0.1 / 0.1	<b>100</b>	Constant/ $v_t=0.1$
<b>ctx155</b>	asymmetry-skewness	YES / 0.1	Wave averaged	<b>0.1 / 0.3</b>	100	Constant/ $v_t=0.1$
<b>ctx144</b>	surface roller-beta	YES / <b>0.07</b>	Wave averaged	0.1 / 0.3	100	Constant/ $v_t=0.1$
<b>ctx162</b>	asymmetry-skewness	YES / <b>0.07</b>	Wave averaged	<b>0.0 / 0.0</b>	100	Constant/ $v_t=0.1$
<b>ctx158</b>	wave turbulence	YES / 0.07	<b>None</b>	0.1 / 0.3	100	Constant/ $v_t=0.1$
<b>ctx159</b>	roller- w. turbulence	<b>NO / -</b>	<b>None</b>	0.1 / 0.3	100	Constant/ $v_t=0.1$
<b>ctx160</b>	roller-turb.-nonlinearity	<b>NO / -</b>	<b>None</b>	<b>0.0 / 0.0</b>	100	Constant/ $v_t=0.1$
<b>ctx166</b>	subgrid turb. model	YES / 0.07	Wave averaged	0.1 / 0.3	100	<b>Smag/nski <math>C_s=0.1</math></b>

The first parameter to be calibrated was the ratio between near-bed concentration and the mean concentration  $R_{cs}$  (run ctx165), which regulates the temporal response of sediment motion to the disturbing forces (adaptation time). Large values of  $R_{cs}$  correspond to small adaptation time and hence lead to quicker bottom changes caused by the imposed bed stresses. Then, wave non-linearity influence is tested through the calibration of the factors  $f_{AS}$  for the wave asymmetry and  $f_{SK}$  for the wave skewness (run ctx155). The contribution of surface rollers, which is adjusted by the breaker slope coefficient  $\beta$ , is then investigated (run ctx144). There are also experiments where one or more mechanisms are deactivated so that the relative influence of each of them to be studied easier (runs ctx162, ctx158, ctx159, ctx160). Specifically, there are tests in which:

- wave nonlinearity is deactivated (run ctx162),
- wave breaking near-bed turbulence is deactivated (run ctx158),
- both surface rollers & wave breaking near-bed turbulence are deactivated (run ctx159),
- only Stokes drift is activated (ctx160)

In Figure 14, the modelled bed evolution for the calibrated wave breaking model (Table 7) and the optimal XBeach settings from the OG case (run ctx144), is presented against the measured bed level at the end of OG phase, in order to get a general view of the model's performance in erosive conditions. In general, the model is capable of predicting the sandbar migration to the offshore very good, although the height of the sandbar in the simulation is somewhat smaller than the measured one. Obviously the model predicts moderate erosion close to the shoreline, finding which is not in agreement with the measurements.

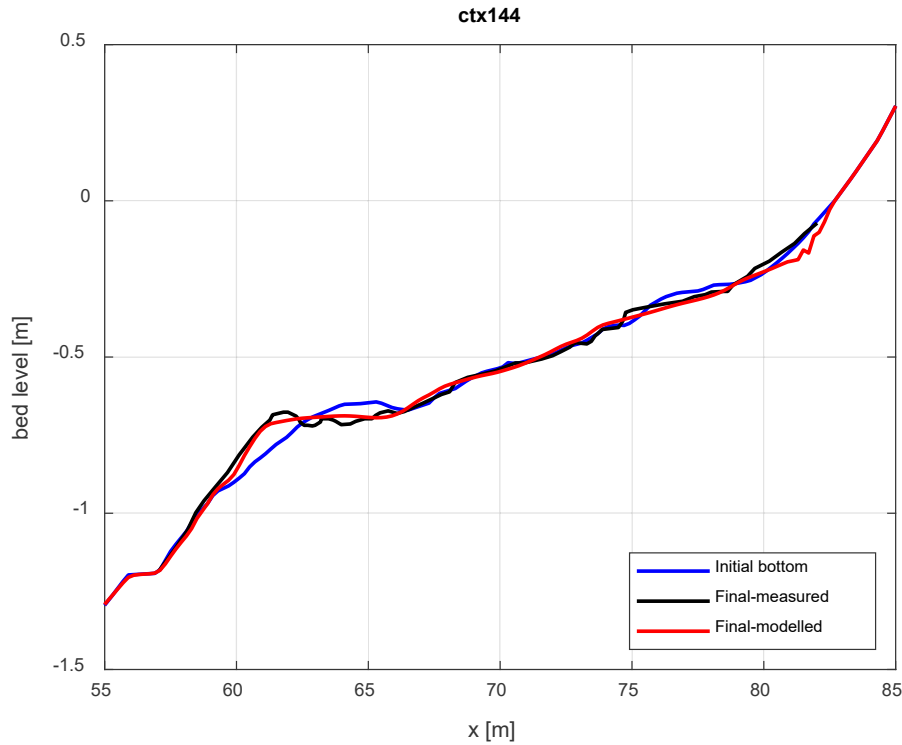


Figure 14: Measured and modelled bottom evolution at the end of the OG phase for the run with the optimal settings (ctx144).

In Figure 15, the total bed level change at the end of the simulation period of OG phase for the runs included in Table 8, is presented. The main findings are:

- The default value of the concentration ratio  $R_{cs}$  (=1) leads to rather diffusive bed evolution, while a value two orders of magnitude higher leads to a clear offshore migration of the sandbar (see also Figure 16). A test with  $R_{cs}$  =10 (not presented here) led to only slightly more diffusive results compared to those of  $R_{cs}$  =100.
- Increased wave non-linearity (through skewness calibration factor) seems to have a positive impact as it restricts the unwanted diffusion of the weather side of migrated sandbar to the offshore.
- Decreasing breaker slope coefficient  $\beta$  enhances the offshore sandbar formation, but also the erosion close to the shoreline.
- Deactivation of wave non-linearity allows sandbar to move offshore (to larger depth than expected) much easier (see also Figure 17) .
- The impact of wave breaking turbulence is noticeable for the sandbar migration to the offshore.
- Minor bed level changes occur when rollers are deactivated and wave non-linearity is activated.
- Opposite to what was observed in the corresponding XBeach simulation, return flow itself (surface rollers, turbulence and wave non-linearity deactivated) results into total erosion of the initial sandbar, which is diffused in larger depths (see also Figure 18).

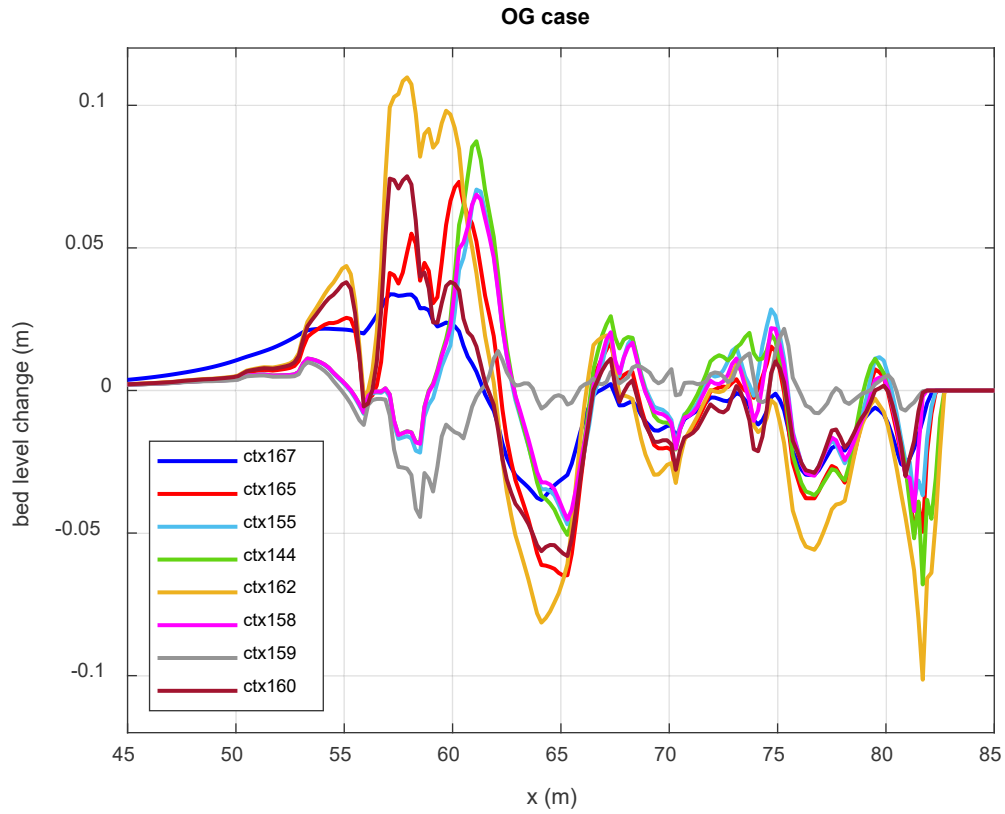


Figure 15: Total bed level change at the end of the GAIA simulations for the runs of Table 8 [OG case].

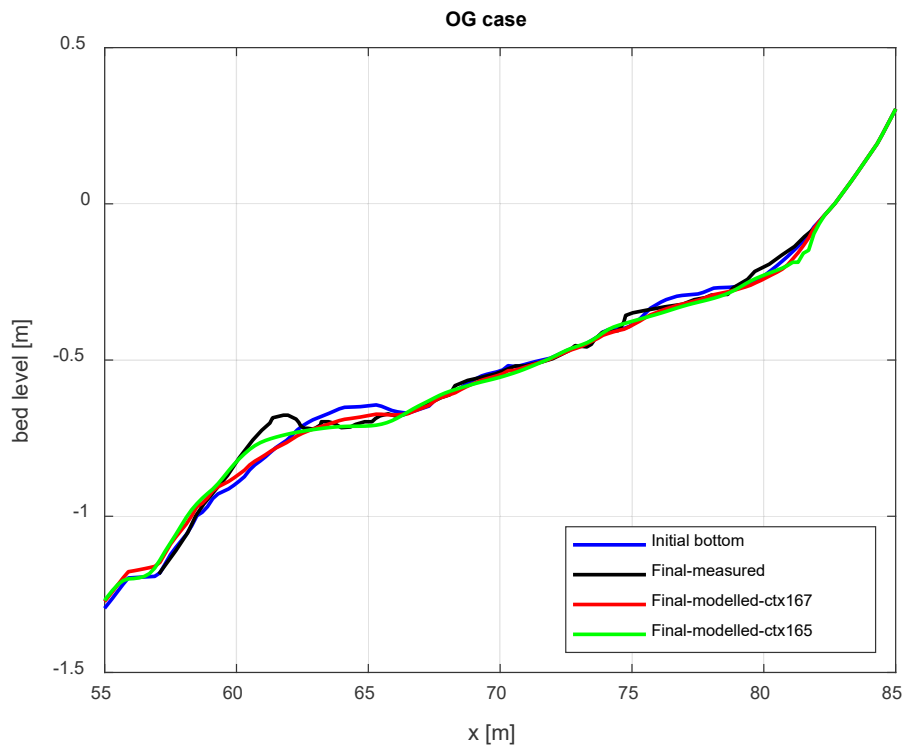


Figure 16: Measured and modelled bottom evolution at the end of the OG phase for the runs with different  $R_{cs}$  values.

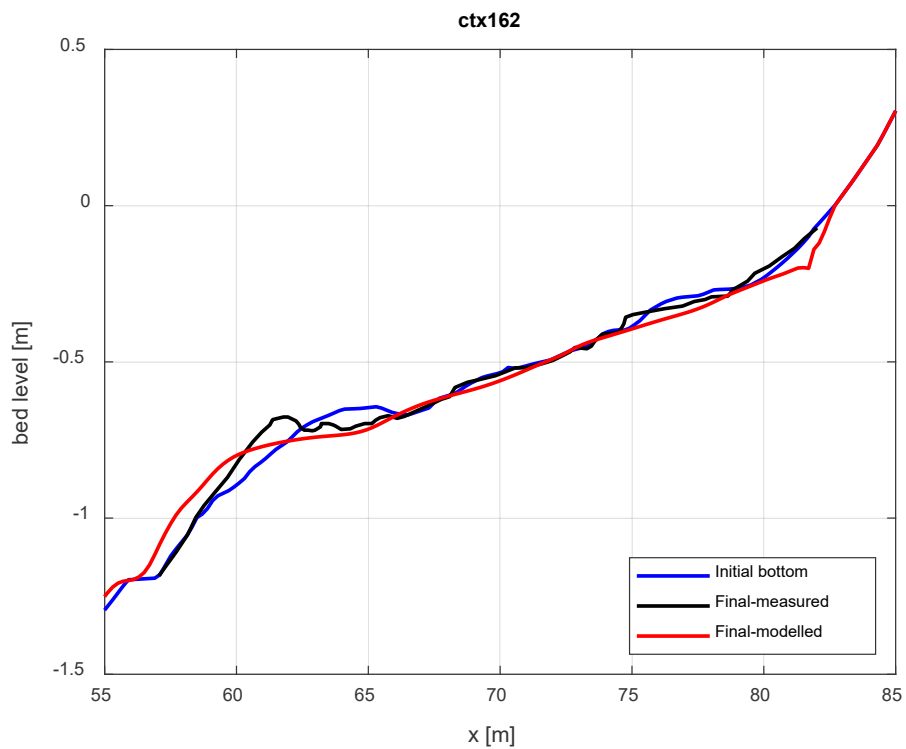


Figure 17: Measured and modelled bottom evolution at the end of the OG phase for the run with deactivated wave non-linearity.

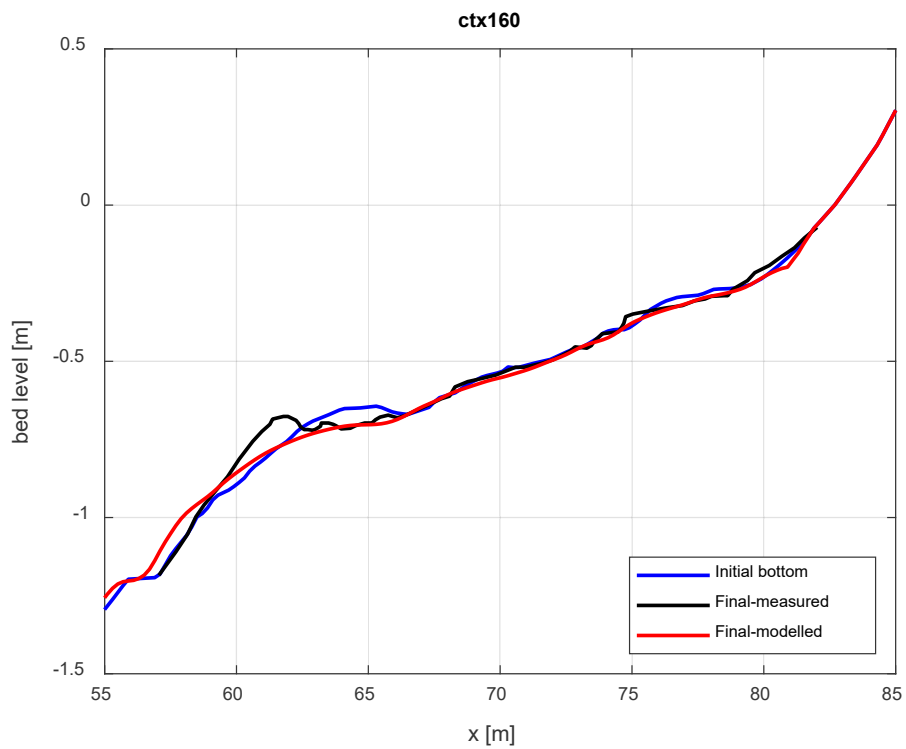


Figure 18: Measured and modelled bottom evolution at the end of the OG phase for the run with only return flow activated.

In the last test mentioned in Table 8, the effect of using the Smagorinski subgrid model instead of considering constant horizontal viscosity ( $\nu_t = 0.1 \text{ m}^2/\text{s}$ ), was investigated. As shown in Figure 19, the Smagorinski model seems to disturb substantially the uniformity of the bed evolution in the transverse direction, especially at the area close to the south boundary of the domain, between  $55 \text{ m} < x < 75 \text{ m}$ . It is conjectured that this (unwanted) behavior is favoured by the enhanced turbulent viscosity.

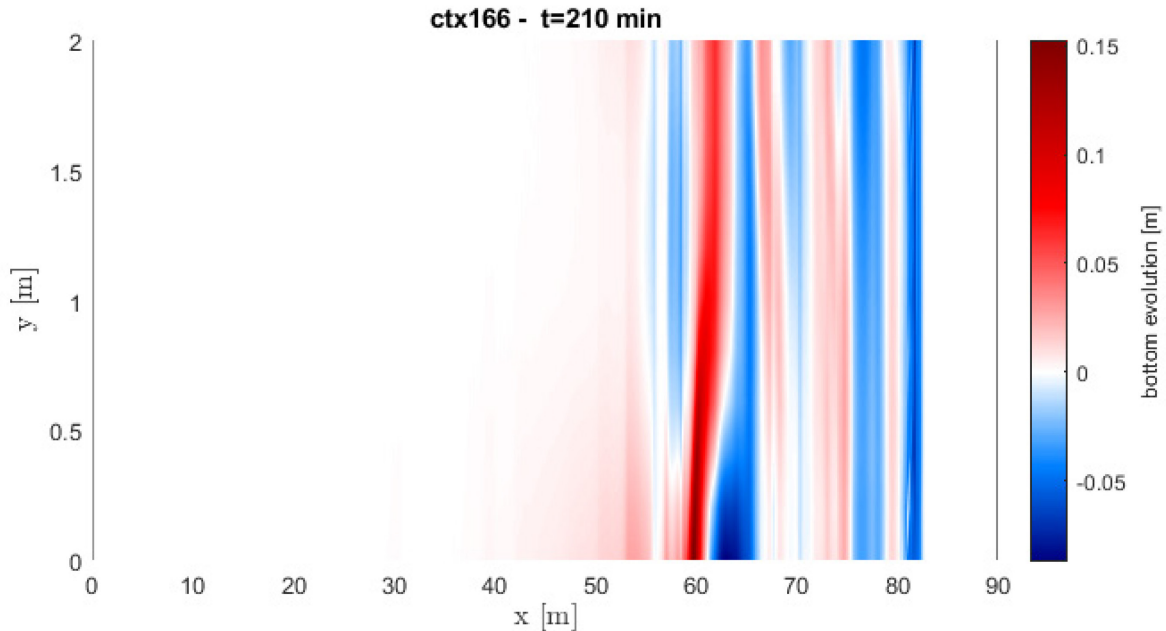


Figure 19: Modelled bottom evolution at the end of the OG phase for the run with the Smagorinski model activated.

Figure 20 shows the modelled by the optimal run (ctx144) wave setup, undertow velocity, wave-velocity skewness  $Sk$ , wave-velocity asymmetry  $As$ , sediment concentration and total transport rate, against corresponding measured data. Reasonable model-data agreement can be observed for the wave setup, the asymmetry  $As$ , the sediment concentration (for  $x < 65 \text{ m}$ ), and for the total transport rate overall. Skewness  $Sk$  is rather overestimated by the model at the area of the sandbar. As for the undertow velocity (positive values indicate offshore direction), model and measured data are in good agreement when wave non-linearity contribution is omitted by the mean advection velocity  $U_E$ , i.e. only Stokes drift  $U_{ST}$  and surface roller  $U_{SR}$  are taken into account, otherwise the model predictions seem to be rather underestimated.

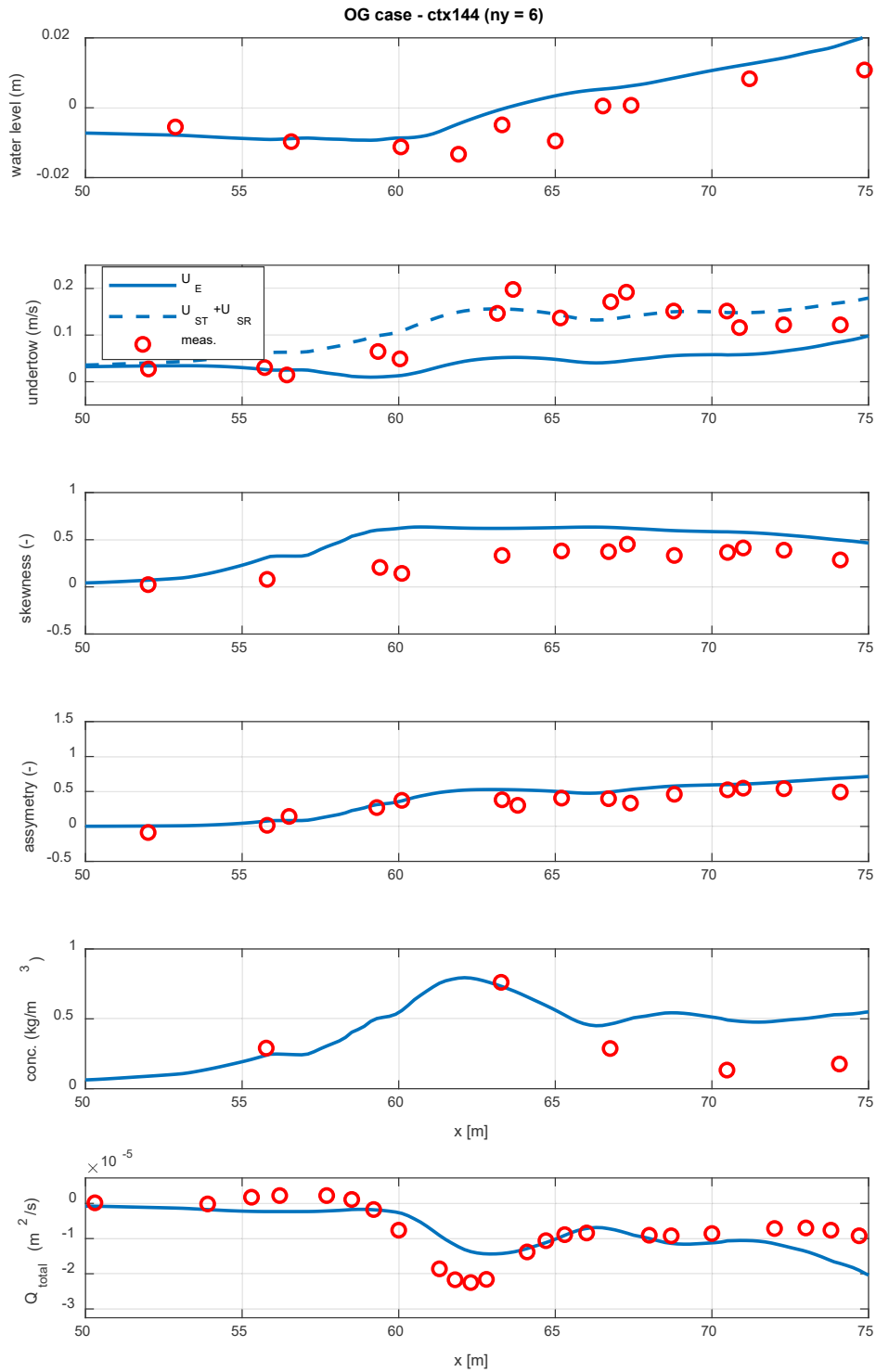


Figure 20: Measured (red circles) and modelled (blue lines) results for the run with the optimal settings (ctx144) for the OG case.

### 4.3 Middle Sandbar Generation (MG) case

Wave breaking calibration takes place first also for the MG case, which corresponds to milder wave conditions (accretive). As in the OG case, during the wave breaking calibration the bottom is considered as frozen and the utilized wave breaking is the one proposed by Battjes & Janssen (1978). The values of the basic tuning parameters of Battjes & Janssen model (JB78), before and after calibration, are shown in Table 9. Note that the calibrated in the OG case values are also given in the same table. The cross-shore variation of significant wave height ( $H_s$ ) for the considered versions of the JB78 model against the measurements are shown in Figure 21. It seems that OG calibrated results for the  $H_s$  dissipation are close to the ones of the default JB78 model. The small differences are attributed to the different value of the ALPHA coefficient rather than the difference in the GAMMA1 (less sensitive coefficient). As for the MG calibrated parameters, which are finally preferred, it seems that a lower value for the GAMMA2 coefficient results in to larger dissipation an better agreement with the (highest) measured values.

Table 9: Calibrated parameters of Battjes & Janssen wave breaking model (1978) for the MG case.

JB78 parameters	default	calibrated-OG	calibrated-MG
$H_m$ COMPUTATION METHOD	1	2	2
BREAKING BJ COEFFICIENT GAMMA1	0.88	<b>0.80</b>	<b>0.80</b>
BREAKING BJ COEFFICIENT GAMMA2	0.80	0.80	<b>0.70</b>
BREAKING BJ COEFFICIENT ALPHA	1.00	<b>0.80</b>	<b>0.80</b>

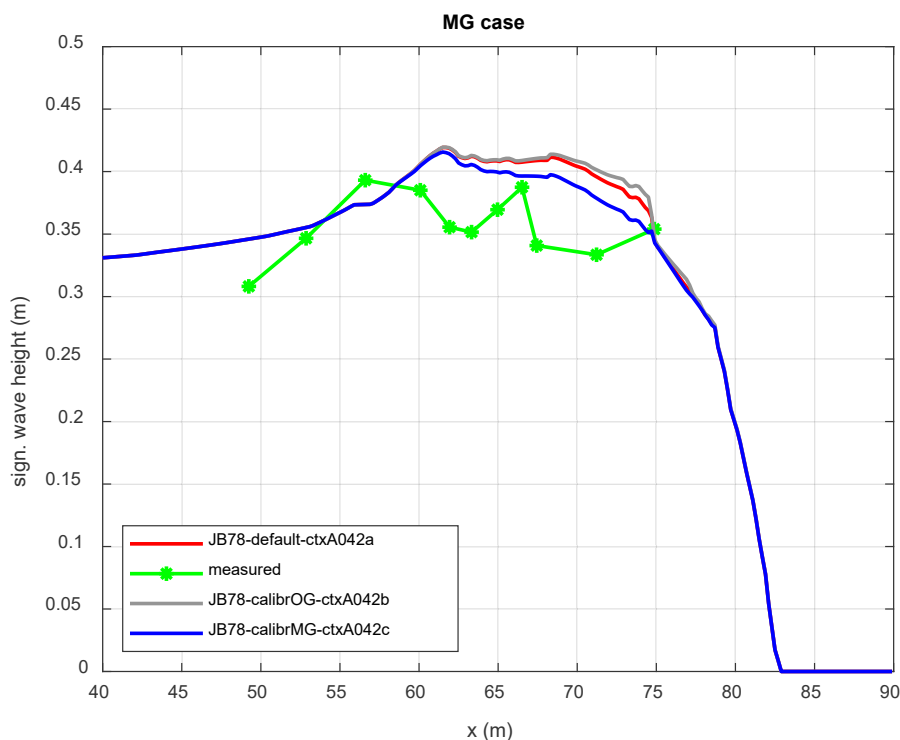


Figure 21: Modelled by TOMAWAC significant wave height variation at the breaking zone and the surf zone for the CROSSTEX experiment [MG case].



Then, as for the OG phase, a series of sensitivity tests (runs) for the main mechanisms that drive cross-shore sediment transport was performed considering movable bed and simulation period equal to the duration of the MG phase. The parameters of the morphological simulations are summarized in Table 10. The investigated parameters are: the GAMMA2 factor (wave breaking), the *beta* parameter (surface rollers), the asymmetry and skewness parameters (wave non-linearity) and the concentration ratio  $R_{cs}$ . Tests with deactivated surface rollers and wave breaking turbulence are also performed in order to investigate the sole effect of wave-nonlinearity, which causes onshore transport, under accretive wave conditions.

Table 10: GAIA & TOMAWAC parameters and processes investigated in sensitivity tests for the MG case.

Run	Tuned parameter	GAIA-TOMAWAC parameter				
		GAMMA2	Roller/beta	Wave turbulence	$f_{As} / f_{Sk}$	$R_{cs}$
ctxA047	settings identical to ctx144	0.8	YES / 0.07	Wave averaged	0.1 / 0.3	100
ctxA050	wave breaking—GAMMA2	<b>0.7</b>	YES / 0.07	Wave averaged	0.1 / 0.3	100
ctxA054	asymmetry	0.7	YES / 0.07	Wave averaged	<b>0.3</b> / 0.3	100
ctxA051	skewness	0.7	YES / 0.07	Wave averaged	0.3 / <b>0.1</b>	100
ctxA056	concentration ratio $R_{cs}$	0.7	YES / 0.07	Wave averaged	0.3 / 0.1	<b>1</b>
ctxA058	surface roller-beta	0.7	YES / <b>0.15</b>	Wave averaged	0.3 / 0.1	1
ctxA060	wave turbulence	0.7	YES / 0.07	<b>None</b>	0.3 / 0.1	1
ctxA059	roller- w. turbulence	0.7	<b>NO</b> / -	<b>None</b>	0.3 / 0.1	1

In Figure 22, the modelled bed evolution at the end of the MG phase for the two first tests (ctxA047 & ctxA050), which make use of the model settings from the OG experiment, are presented. Obviously, the difference in the wave breaking calibration affects the bed level change for  $x > 65$  m. The less dissipative wave breaking (ctxA047) leads to larger erosion and instabilities close to the shoreline, therefore the wave breaking settings of ctxA050 are considered in the following tests. Compared to the measured bed level, the numerical predictions show relatively poor performance of the model. Even though the prediction of eroding shallow bed and gathering and accumulation of sediment between  $65 \text{ m} < x < 70 \text{ m}$  seems to be promising, on the other hand the model fails to predict the erosion of the offshore sandbar.

The sensitivity of the numerical results to the wave non-linearity factors, i.e.  $f_{As}$  for the wave asymmetry and  $f_{Sk}$  for the wave skewness, is presented in Figure 23. Obviously, the influence of wave asymmetry on the bed evolution, is larger compared to the influence of wave skewness. Increasing  $f_{As}$  (test ctxA054) causes onshore migration of the offshore sandbar but, on the other hand, reduces erosion close to the shoreline and hence it restricts the accumulated sediment to shallower depths compared to the reference test ctxA050. As for the skewness factor  $f_{Sk}$ , it seems that reducing its value (keeping  $f_{As}$  high) doesn't affect the onshore transport to the extent that wave asymmetry does (ctxA051).

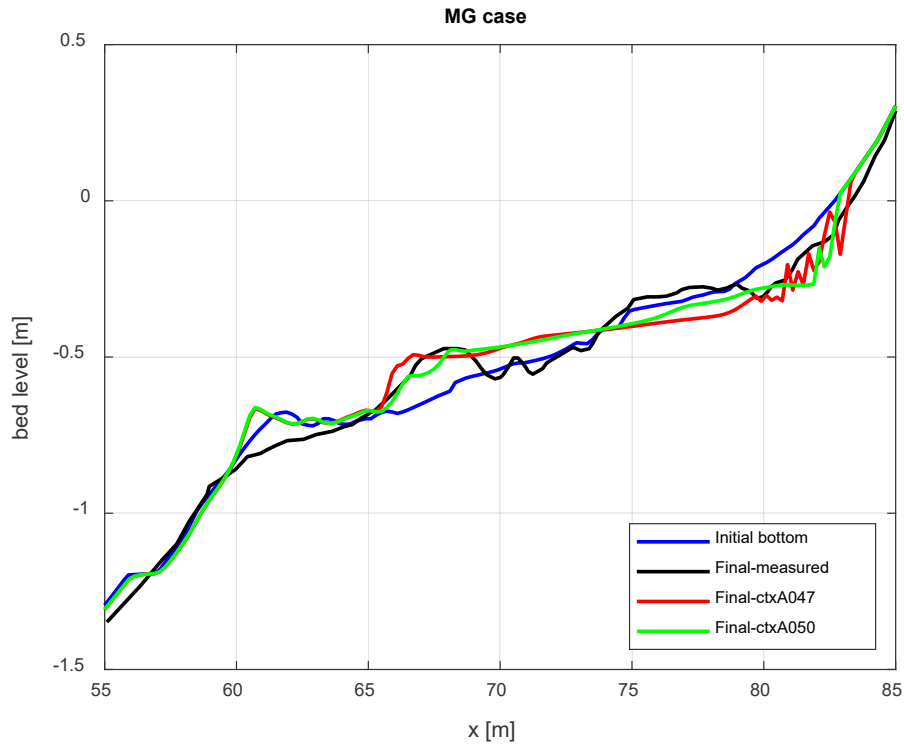


Figure 22: Measured and modelled bottom evolution at the end of the MG phase for the runs ctxA047 & ctxA050 (see Table 10).

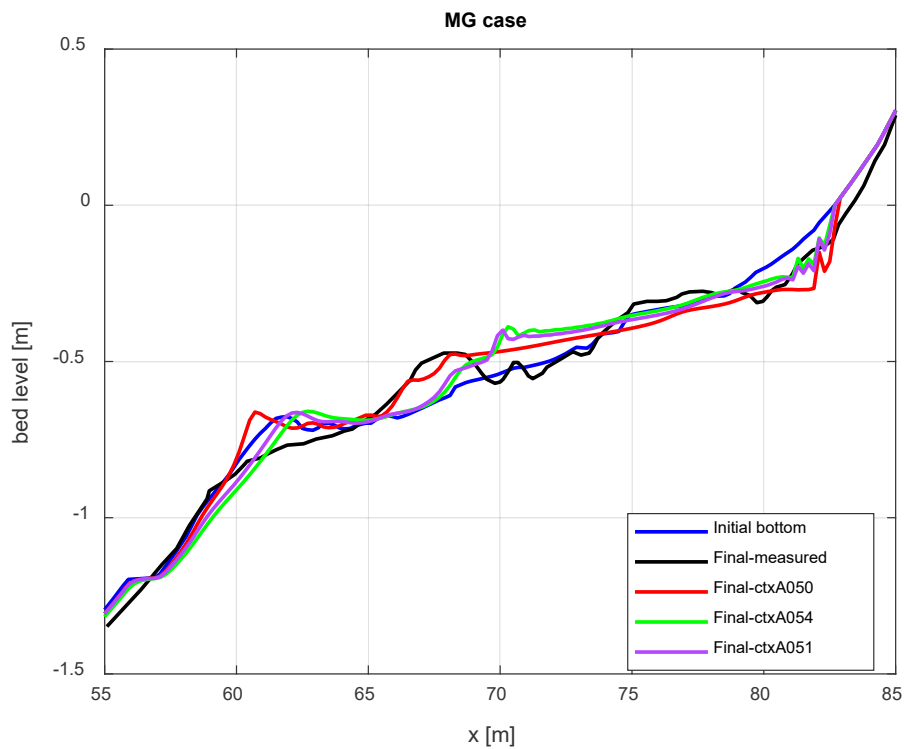


Figure 23: Measured and modelled bottom evolution at the end of the MG phase for the runs of wave non-linearity calibration.

The concentration ratio  $R_{cs}$  turns out to be a rather important factor also in bed evolution under accretive conditions, presenting though the opposite behavior compared to the erosive (OG) case. As shown in Figure 24, reduction the  $R_{cs}$  by two order of magnitude, minimizes the unwanted erosion of the deeper bottom part ( $x < 60$  m), while letting the offshore sandbar to be smoothed out easier. Moreover it diminishes the instabilities at the deepening area close the shoreline and assists into a smoother accumulation of sediment close to the area of the measured middle sandbar.

In Figure 25, the sensitivity of the bed evolution to the adjustment of the *beta* factor of the surface rollers, is presented. It seems that, increasing substantially the value of *beta*, decreases the erosion of the bottom close to the shoreline and hence the amount of sediment moving offshore, while it has negligible impact on the evolution of the offshore sandbar.

The sensitivity of the numerical results to the deactivation of wave turbulence (run ctxA060) and the deactivation of both surface rollers and wave turbulence (ctxA059), is depicted in Figure 26. It seems that the effect of wave induced turbulence is relatively important at very shallow waters, where it enhances erosion. Consequently, it affects the amount of the accumulated sediment to deeper. Bed evolution under the action of only two of the considered cross-shore mechanisms, i.e. the return flow and the wave nonlinearity, presents substantial differences to medium and shallow water depths. Apart from the observed instabilities, the model exhibits low activity at the shallow areas (no erosion at the shoreline – limited accumulation of sediment at depths around 0.5 m), while it is confirmed that the surface rollers have minimal impact at the offshore sandbar area.

Taking into account the findings of the calibration/validation tests, in general, the model is not capable of predicting a clear middle sandbar formation, as found in the laboratory experiments. However, it is capable of predicting partial erosion of the offshore sandbar, the erosion at shallow water and the accumulation of sediment at the area of the measured middle sandbar.

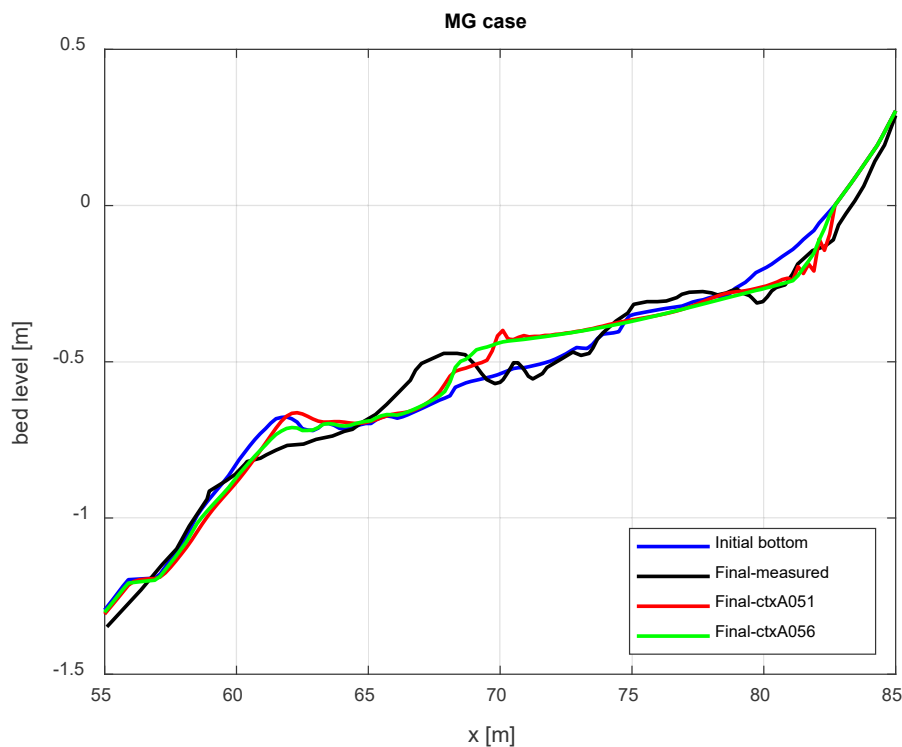


Figure 24: Measured and modelled bottom evolution at the end of the MG phase for the runs of concentration ratio  $R_{cs}$  calibration.

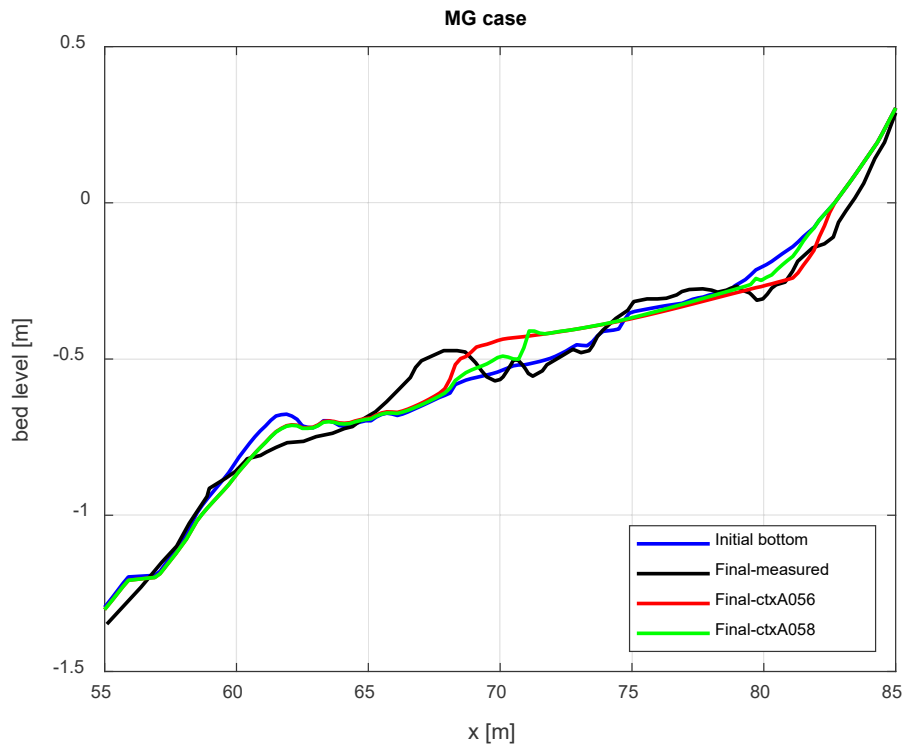


Figure 25: Measured and modelled bottom evolution at the end of the MG phase for the runs of beta factor (surf roller) calibration.

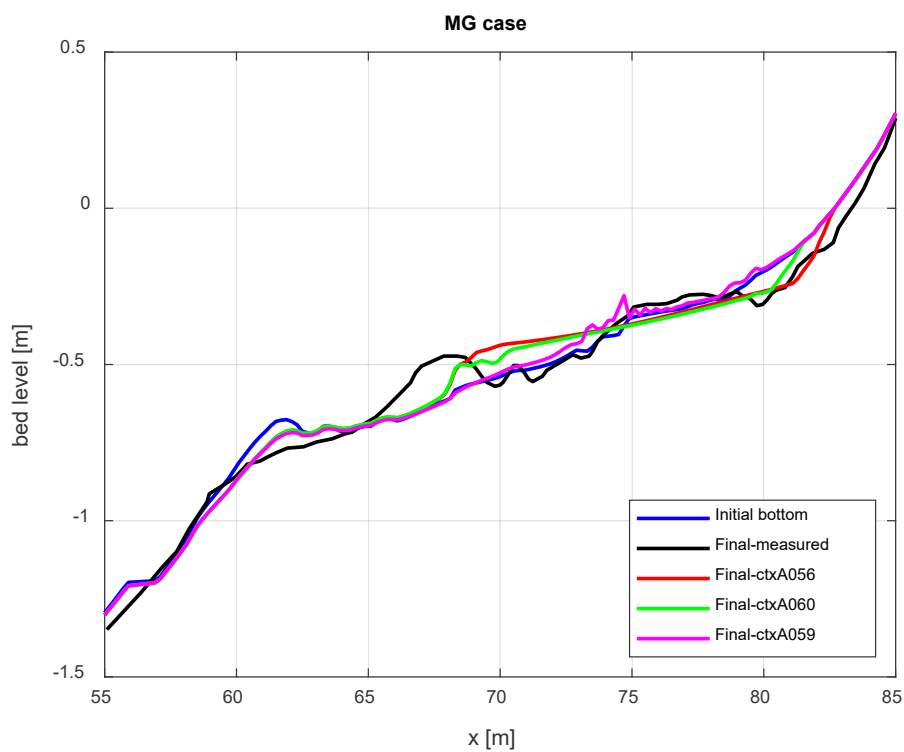


Figure 26: Measured and modelled bottom evolution at the end of the MG phase for the runs with deactivated wave turbulence (ctxA060) and deactivated surface rollers + wave turbulence (ctxA059).

Figure 27 shows the modelled by the optimal run (ctxA056) wave setup, undertow velocity, wave-velocity skewness  $Sk$ , wave-velocity asymmetry  $As$ , sediment concentration and total transport rate, against corresponding measured data. Reasonable model-data agreement can be observed for the wave setup, the asymmetry  $As$ , the sediment concentration (only for  $x < 68$  m), and for the total transport rate for  $x < 71$  m. Agreement with skewness  $Sk$  is fair. As for the undertow velocity (positive values indicate offshore direction), model and measured data are in good agreement, when wave non-linearity contribution is omitted by the mean advection velocity  $U_E$ , i.e only Stokes drift  $U_{ST}$  and surface roller  $U_{SR}$  are taken into account, otherwise the model predictions seem to be rather underestimated, as also observed in the OG case.

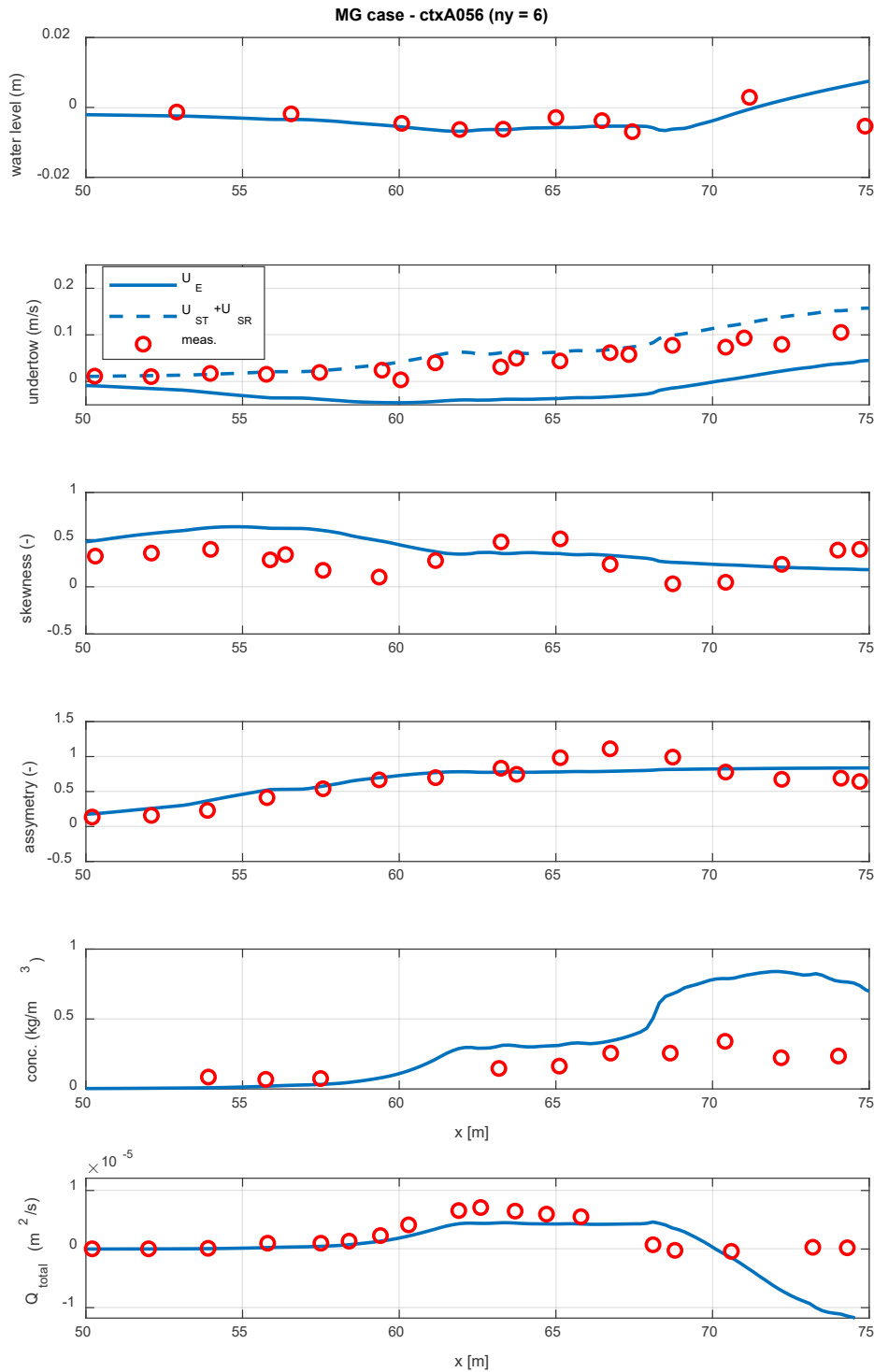


Figure 27: Measured (red circles) and modelled (blue lines) results for the run with the optimal settings (ctxA056) for the MG case.

## 5 Conclusions

The implementation of major cross-shore processes, i.e the Stokes drift, the surface rollers, the wave non-linearity and the wave breaking induced turbulence, in the TOMAWAC and GAIA modules, was the main subject of this work. Prior to this, the XBeach model was utilized for the reproduction of the results of a well known large scale laboratory experiment (CROSSTEX), in order to evaluate the importance of each cross-shore process, before they are implemented in the corresponding modules of TELEMAC. Both models, Xbeach and TELEMAC (GAIA), were calibrated/validated based on the reproduction of the measured data under both storm (erosive) and mild (accretive) wave conditions.

For the erosive conditions, XBeach model was capable of predicting the offshore sandbar migration fairly good, although the height of the sandbar was found considerably smaller than the measured one. The model predicted limited erosion close to the shoreline, which was not observed in the measurements. As for the accretive conditions, XBeach model failed in predicting the middle sandbar generation, even though an onshore migration of the offshore sandbar could be reproduced. Furthermore, the model underestimated the measured erosion at shallow depths ( $< 0.3$  m).

GAIA found to be capable of predicting the sandbar migration to the offshore very good, although the height of the sandbar was found somewhat smaller than the measured one (erosive conditions). The model predicted moderate erosion close to the shoreline, finding which was in accordance with the measurements.

As for the accretive case, GAIA faced difficulties in predicting a clear middle sandbar formation, as it was found in the laboratory experiment. However, it was capable of predicting partial erosion of the offshore sandbar, the erosion at shallow water and the accumulation of sediment at the area of the measured middle sandbar.

Taking into account the findings of the calibration/validation tests for both models, it was concluded that TELEMAC presents better behavior in reproducing cross-shore transport under both erosive and accretive conditions, compared to the XBeach model. Note that the comparison was based on the utilization of similar formulations for the considered processes by both models. XBeach offers more options for specific processes, such as for the transformed wave shape and the wave-induced turbulence, which were not considered in the present work.

## References

- Baldock, T. E., Holmes, P., Bunker, S., & Van Weert, P. (1998). Cross-shore hydrodynamics within an unsaturated surf zone. *Coastal Engineering*, 34(3), 173–196. [https://doi.org/https://doi.org/10.1016/S0378-3839\(98\)00017-9](https://doi.org/https://doi.org/10.1016/S0378-3839(98)00017-9)
- Battjes, J. A., & Janssen, J. (1978). *ENERGY LOSS AND SET-UP DUE TO BREAKING OF RANDOM WAVES*. <https://api.semanticscholar.org/CorpusID:117201527>
- Cobo, P. T., Kirby, J. T., Haller, M. C., Ozkan-Haller, H. T., Magallen, J., & Guannel, G. (2007). MODEL SIMULATIONS OF BAR EVOLUTION IN A LARGE SCALE LABORATORY BEACH. *Coastal Engineering 2006*, 2566–2578. [https://doi.org/doi:10.1142/9789812709554\\_0217](https://doi.org/doi:10.1142/9789812709554_0217)
- Fonias, E., Breugem, W. A., Wang, L., Wang, L., Bolle, A., Kolokythas, G., & De Maerschalck, B. (2021). Implementation of cross-shore processes in GAIA. In *Proceedings of the papers submitted to the 2020 TELEMAT-MASCARET user conference - October 2021* (pp. 138–143). [S.n.]. <http://0.5.78.221>
- Guannel, G. E. (2009). *Observations of Cross-Shore Sediment Transport and Formulation of the Undertow* [PhD Thesis]. Oregon State University.
- Janssen, T. T., & Battjes, J. A. (2007). A note on wave energy dissipation over steep beaches. *Coastal Engineering*, 54(9), 711–716. <https://doi.org/https://doi.org/10.1016/j.coastaleng.2007.05.006>
- Roelvink, J. A. (1993). Dissipation in random wave groups incident on a beach. *Coastal Engineering*, 19(1), 127–150. [https://doi.org/https://doi.org/10.1016/0378-3839\(93\)90021-Y](https://doi.org/https://doi.org/10.1016/0378-3839(93)90021-Y)
- Roelvink, J. A., & Stive, M. J. F. (1989). Bar-generating cross-shore flow mechanisms on a beach. *Journal of Geophysical Research: Oceans*, 94(C4), 4785–4800. <https://doi.org/https://doi.org/10.1029/JC094iC04p04785>
- Ruessink, B. G., Miles, J. R., Feddersen, F., Guza, R. T., & Elgar, S. (2001). Modeling the alongshore current on barred beaches. *Journal of Geophysical Research: Oceans*, 106(C10), 22451–22463. <https://doi.org/https://doi.org/10.1029/2000JC000766>
- Soulsby, R. (1997). *Dynamics of marine sands*. H.R. Wallingford.
- Svendsen, I. A. (1984a). Mass flux and undertow in a surf zone. *Coastal Engineering*, 8(4), 347–365. [https://doi.org/https://doi.org/10.1016/0378-3839\(84\)90030-9](https://doi.org/https://doi.org/10.1016/0378-3839(84)90030-9)
- Svendsen, I. A. (1984b). Wave heights and set-up in a surf zone. *Coastal Engineering*, 8(4), 303–329. [https://doi.org/https://doi.org/10.1016/0378-3839\(84\)90028-0](https://doi.org/https://doi.org/10.1016/0378-3839(84)90028-0)
- van Thiel de Vries, J. S. M. (2009). Dune erosion during storm surges [PhD Thesis]. In *Delft, the Netherlands, Delft Hydraul. Lab., Sep. 2009*.

DEPARTMENT **MOBILITY & PUBLIC WORKS**  
Flanders hydraulics

Berchemlei 115, 2140 Antwerp

**T** +32 (0)3 224 60 35

**F** +32 (0)3 224 60 36

[flanders.hydraulics@vlaanderen.be](mailto:flanders.hydraulics@vlaanderen.be)

[www.flandershydraulics.be](http://www.flandershydraulics.be)